laser-lok®
microchannels
clinical overview

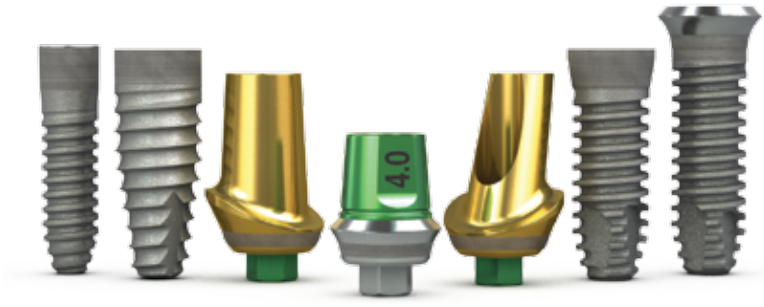

unique technology for unique results

BIOHORIZONS®

SCIENCE • INNOVATION • SERVICE

BIOHORIZONS®

99.2% average implant success rate[1]

BioHorizons is dedicated to developing evidence-based and scientifically proven products. From the launch of the External implant system (Maestro) in 1997, to the Laser-Lok 3.0 implant in 2010, dental professionals as well as patients have confidence in our comprehensive portfolio of dental implants and biologics products.

Our commitment to science, innovation and service has aided us in becoming one of the fastest growing companies in the dental industry. BioHorizons has helped restore smiles in 85 markets throughout Asia, North America, South America, Africa, Australia and Europe.

global leader for biologic based solutions

SCIENCE

BioHorizons uses science and innovation to create unique products with proven surgical and esthetic results.

INNOVATION

Our advanced implant technologies, biologic products and computer guided surgery software have made BioHorizons a leading dental implant company.

products sold in 85 markets

SERVICE

BioHorizons understands the importance of providing excellent service. Our global network of professional representatives and our highly trained customer care support team are well-equipped to meet the needs of patients and clinicians.

Study Review

The following review presents some of the studies and presentations related to Laser-Lok microchannels.

Latest Research

Human Studies

Development Research

BIOHORIZONS®

Laser-Lok Technology

Laser-Lok overview

Laser-Lok microchannels is a proprietary dental implant surface treatment developed from over 20 years of research initiated to create the optimal implant surface. Through this research, the unique Laser-Lok surface has been shown to elicit a biologic response that includes the inhibition of epithelial downgrowth and the attachment of connective tissue (unlike Sharpey fibers).[2,3] This physical attachment produces a biologic seal around the implant that protects and maintains crestal bone health. The Laser-Lok phenomenon has been shown in post-market studies to be more effective than other implant designs in reducing bone loss.[4,5,6,7]

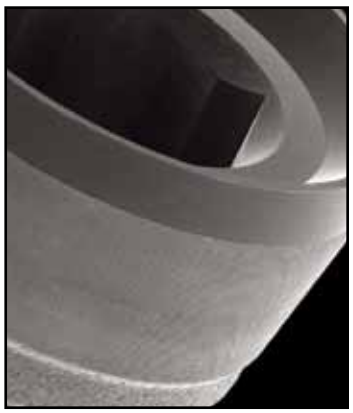

SEM image at 30X showing the Laser-Lok zone on a BioHorizons implant.

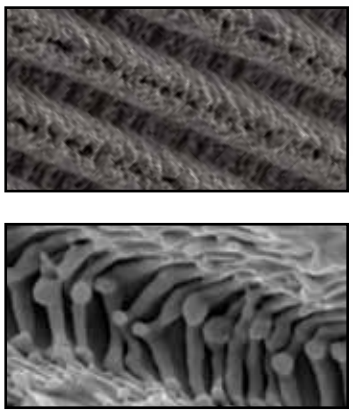

The uniformity of the Laser-Lok microstructure and nanostructure is evident using extreme magnification.

Unique surface characteristics

Laser-Lok microchannels is a series of cell-sized circumferential channels that are precisely created using laser ablation technology. This technology produces extremely consistent microchannels that are optimally sized to attach and organize both osteoblasts and fibroblasts.[8,9] The Laser-Lok microstructure also includes a repeating nanostructure that maximizes surface area and enables cell pseudopodia and collagen microfibrils to interdigitate with the Laser-Lok surface.

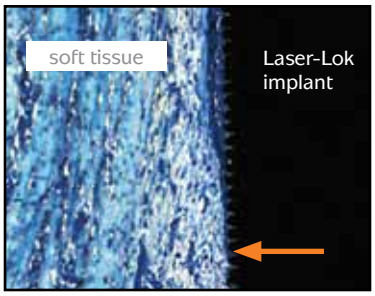

Human histology shows the apical extent of the junctional epithelium below which there is a supracrestal connective tissue attachment to the Laser-Lok surface.[2]

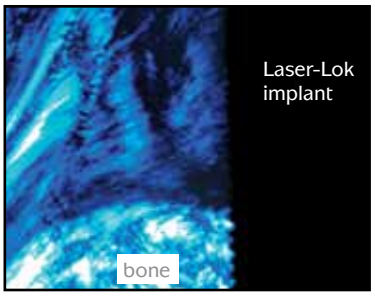

Polarized lights show the connective tissue is functionally oriented.[2]

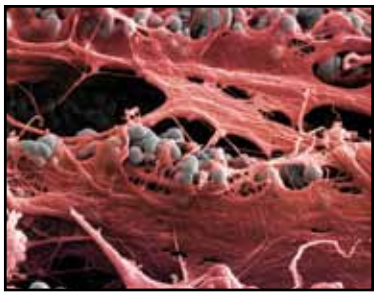

Colorized SEM of a dental implant harvested at 6 months post-op shows the connective tissue is physically attached and interdigitated with the Laser-Lok surface.

Different than other surface treatments

Virtually all dental implant surfaces on the market are grit-blasted and/or acid-etched. These manufacturing methods create random surfaces that vary from point to point on the implant and alter cell reaction depending on where each cell comes in contact with the surface.[10] While random surfaces have shown higher osseointegration than machined surfaces,[11] only the Laser-Lok surface has been shown using light microscopy, polarized light microscopy and scanning electron microscopy to also be effective for soft tissue attachment.[2,12]

The clinical advantage

The Laser-Lok surface has been shown in several studies to offer a clinical advantage over other implant designs. In a prospective, controlled multi-center study, Laser-Lok implants, when placed alongside identical implants with a traditional surface, were shown at 37 months post-op to reduce bone loss by 70% (or 1.35mm).[4] In a retrospective, private practice study, Laser-Lok implants placed in a variety of site conditions and followed up to 3 years minimized bone loss to 0.46mm.[5] In a prospective, University-based overdenture study, Laser-Lok implants reduced bone loss by 63% versus NobelReplace™ Select.[6]

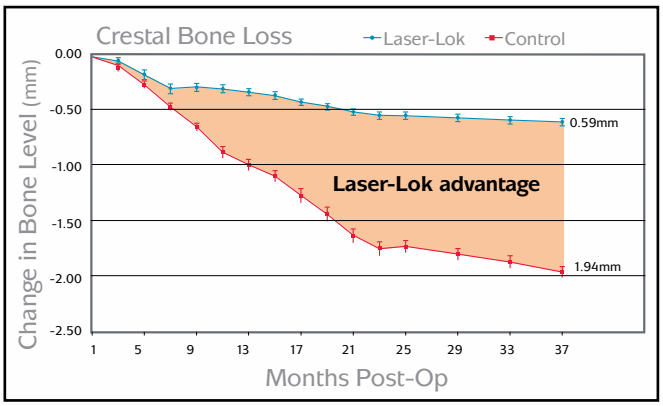

In a 3-year multicenter perspective study, the Laser-Lok surface showed superior bone maintenance over identical implants without the Laser-Lok surface.[4]

Latest discoveries

The establishment of a physical, connective tissue attachment (unlike Sharpey fibers) to the Laser-Lok surface has generated an entirely new area of research and development: Laser-Lok applied to abutments. This could provide an opportunity to use Laser-Lok abutments to create a biologic seal and Laser-Lok implants to establish superior osseointegration[9] – a solution that offers the best of both worlds. Alternatively, Laser-Lok abutments could support peri-implant health around implants without Laser-Lok. In a recent study, Laser-Lok abutments and standard abutments were randomly placed on implants with a grit-blasted surface to evaluate the differences. In this proof-of-principle study, a small band of Laser-Lok microchannels was shown to inhibit epithelial downgrowth and establish a connective tissue attachment (unlike Sharpey fibers) similar to Laser-Lok implants.[12] In these cases, an epithelial barrier and a supracrestal connective tissue barrier were created, even when the implants had a machined collar.[12] The resulting crestal bone levels were higher than what was seen with standard abutments and provides some insight into the role soft tissue stability may play in maintaining crestal bone health.

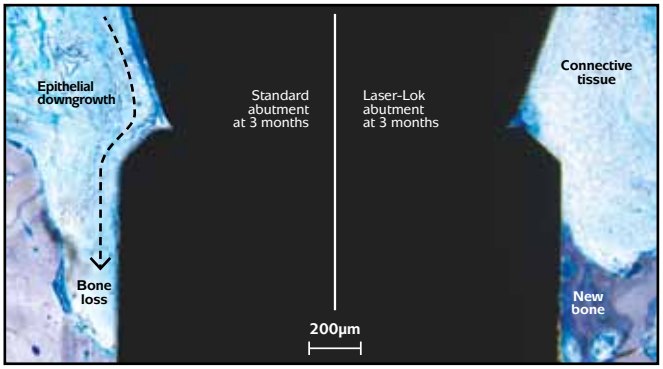

Comparative histologies show the biologic differences between standard abutments and Laser-Lok abutments including changes in epithelial downgrowth, connective tissue and crestal bone health.[12]

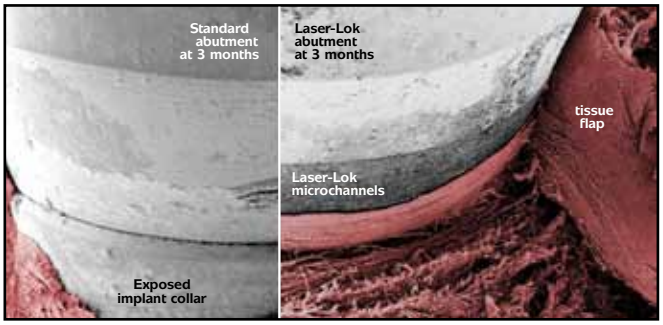

Comparative SEM images show the variation in tissue attachment strength on standard and Laser-Lok abutments when a tissue flap is incised vertically and manually lifted using forceps.[12]

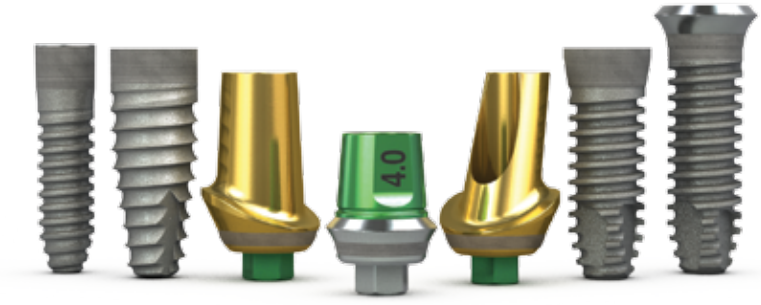

Laser-Lok Technology is available on Laser-Lok 3.0, Tapered Internal, Single-stage, Internal implants & abutments

• *NobelReplace is a trademark of Nobel Biocare.*

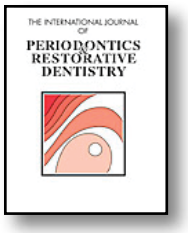

Histologic Evidence of a Connective Tissue Attachment to Laser Microgrooved Abutments: A Canine Study

M Nevins, DM Kim, SH Jun, K Guze, P Schupbach, ML Nevins.
Int J Periodontics Restorative Dent , Volume 30, 2010. p. 245-255.

Standard Abutment

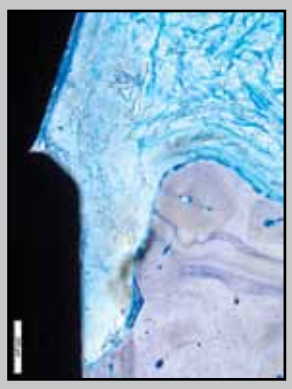

A grit-blasted implant and standard abutment demonstrated apical JE migration, resulting in significant crestal bone resorption.

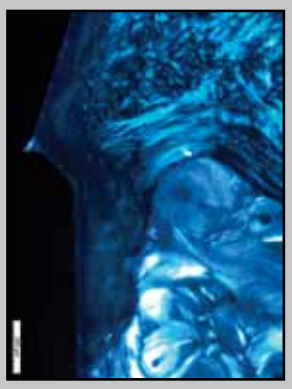

In a polarized light view, this specimen clearly demonstrates parallel running connective tissue fibers against both the abutment and implant collar surfaces. In addition, significant crestal bone loss is seen.

Laser-Lok Abutment

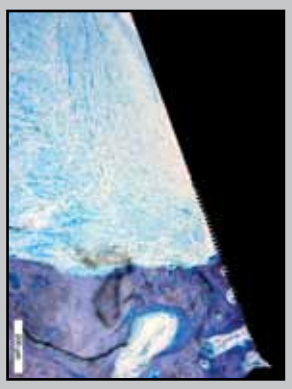

In this specimen, regenerated bone was attached to the Laser-Lok abutment surface and the IAJ microgap was eliminated.

A polarized light image demonstrates perpendicularly inserting connective tissue fibers into the microgrooved abutment surface.

ABSTRACT

Previous research has demonstrated the effectiveness of laser-ablated microgrooves placed within implant collars in supporting direct connective tissue attachments to altered implant surfaces. Such a direct connective tissue attachment serves as a physiologic barrier to the apical migration of the junctional epithelium (JE) and prevents crestal bone resorption. The current prospective preclinical trial sought to evaluate bone and soft tissue healing patterns when laser-ablated microgrooves are placed on the abutment. A canine model was selected for comparison to previous investigations that examined the negative bone and soft tissue sequelae of the implant-abutment microgap. The results demonstrate significant improvement in peri-implant hard and soft tissue healing compared to traditional machined abutment surfaces.

MATERIALS AND METHODS

The current study was designed to examine the effects of two different implant and abutment surfaces on epithelial and connective tissue attachment, as well as peri-implant bone levels. Six foxhounds were selected for this study. Each dog received 6 implants in the bilateral mandibular premolar and first molar extraction sites, for a total of 36 implants. The sites were randomly assigned to receive tapered internal implants (BioHorizons) with either resorbable blast texturing (RBT) or RBT with a 0.3mm machined collar. In addition, either machined-surface or Laser-Lok microchannel healing abutments were assigned randomly to each implant. The abutments were placed at the time of surgery.

RESULTS

The presence of the 0.7 mm laser ablated microchanneled zone consistently enabled intense fibroblastic activity to occur on the abutment-grooved surface, resulting in a dense interlacing complex of connective tissue fibers oriented perpendicular to the abutment surface that served as a physiologic barrier to apical JE migration. As a consequence of inhibiting JE apical migration, crestal bone resorption was prevented. Significantly, in two cases bone regeneration coronal to the IAJ and onto the abutment surface occurred, completely eliminating the negative sequelae of the IAJ microgap.

In contrast, abutments devoid of laser-ablated microgrooved surfaces, exhibited little evidence of robust fibroblastic activity at the abutment-tissue interface. A long JE extended along the abutment and implant collar surfaces, preventing formation of the physiologic connective tissue barrier and causing crestal bone resorption. Parallel rather than functionally oriented perpendicular connective tissue fibers apposed the abutment-implant surfaces.

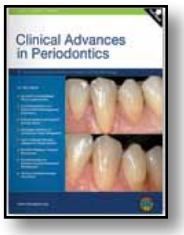

Histologic Evidence of Connective Tissue Integration on Laser Microgrooved Abutments in Humans

NC Geurs, PJ Vassilopoulos, MS Reddy.
Clinical Advances in Periodontics, Vol. 1, No. 1, May 2011.

Ground section of specimen stained with toluidine blue/Azur II. The oral epithelium and junctional epithelium are tapering off coronal to the microgrooved surface.

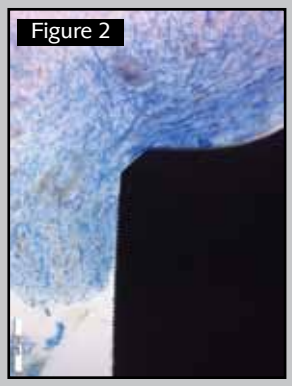

Higher magnification of Figure 1 showing connective tissue in close contact with the microgrooved surface of the abutment.

Polarized light view of Figure 2 demonstrating collagen fibers in a functional orientation toward the abutment surface.

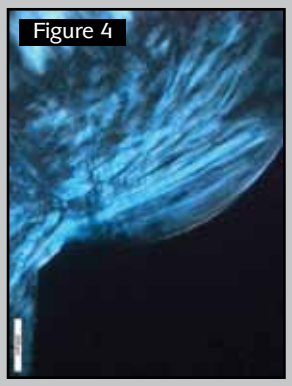

Polarized light view from an area coronal to Figure 3. The orientation of the collagen fibers is more parallel to the smooth implant surface.

INTRODUCTION

Human histology and scanning electron microscopy (SEM) are presented, outlining the soft tissue integration to a laser microgrooved abutment surface.

CASE PRESENTATION

In two patients, prosthetic abutments with a laser microgrooved surface were placed on osseointegrated implants. After 6 weeks of healing, the abutments and the surrounding soft tissue were removed and prepared for histology and SEM. The most apical epithelium was found coronal to this surface. Connective tissue demonstrated collagen fibers oriented perpendicular to the microgrooved surface. There was intimate contact between the connective tissues and the microgrooved abutment surface.

CONCLUSION

The abutments in these patients had connective tissue integration with functionally oriented fibers to the microgrooved surface.

SUMMARY

Why is this case new information? To our knowledge, this is the first human case series reported with human histology describing the connective tissue attachment around a microgrooved abutment.

What are the keys to successful management in this case? The abutment surface characteristics can lead to connective tissue integration with the microgrooved surface, with functionally oriented collagen fibers.

What are the primary limitations to success in this case? This is only a case series of the histology of the attachment. No clinical outcomes or advantages are reported. Further studies will need to be conducted to demonstrate the clinical advantages.

THE INTERNATIONAL JOURNAL OF PERIODONTICS RESTORATIVE DENTISTRY

Connective Tissue Attachment to Laser Microgrooved Abutments: A Human Histologic Case Report

M Nevins, M Camelo, ML Nevins, P Schupbach, DM Kim

Submitted for Publication, Int J Periodontics Restorative Dent

Healing abutments with Laser-Lok microchannels connect to the implant fixtures. Mucoperiosteal flaps closed without tension.

At 10 weeks, healing is normal for patient #1 with no evidence of infection or inflammation.

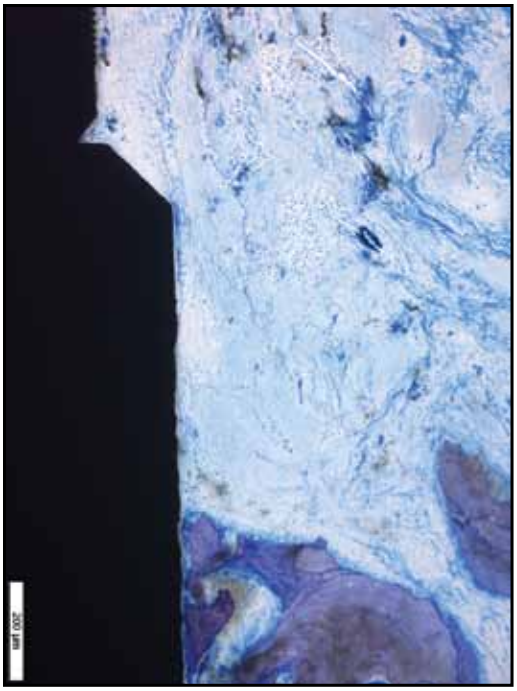

Crestal bone is in close contact with the implant collar surface, with no evidence of bone loss apparent, but rather new bone formation.

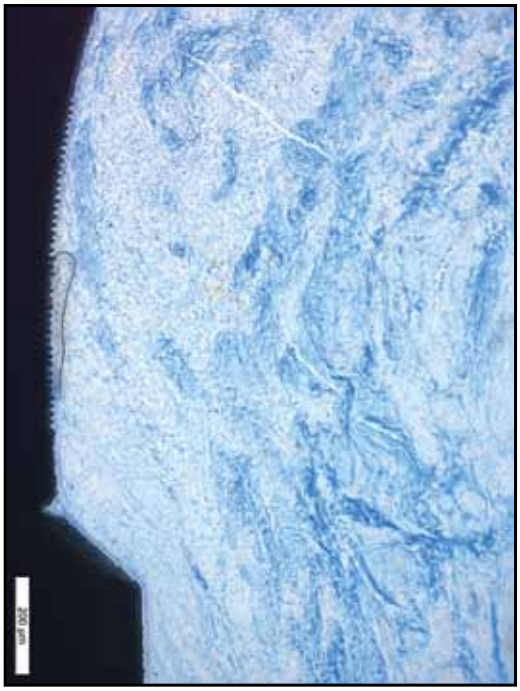

At higher power, dense connective tissue is in intimate contact with the abutment's Laser-Lok micro-grooved surfaces.

ABSTRACT

Previous preclinical and clinical studies have demonstrated the effectiveness of precisely configured laser-ablated microgrooves placed on implant collars to allow direct connective tissue attachment to the implant surface. A recent canine study examining laser-ablated microgrooves placed in a defined healing abutment area demonstrated similar findings. In both instances direct connective tissue attachment to the implant/abutment surface served as an obstacle to the apical migration of the junctional epithelium, thus preventing crestal bone resorption. The current case report examined the effectiveness of abutment positioned laser-ablated microgrooves in human subjects. As in the preclinical trial, precisely defined laser-ablated microgrooves allowed direct connective tissue attachment to the altered abutment surface, prevented apical migration of the junctional epithelium and thus protected crestal bone from premature resorption.

THE INTERNATIONAL JOURNAL OF PERIODONTICS & RESTORATIVE DENTISTRY

Reattachment of the connective tissue fibers to the laser microgrooved abutment surface

M Nevins, M Camelo, ML Nevins, P Schupbach, DM Kim

Submitted for Publication, Int J Periodontics Restorative Dent

Laser microgrooved healing abutments have been placed at the time of the implant surgery.

Laser microgrooved healing abutment has been replaced by the laser microgrooved cylindric permanent abutment.

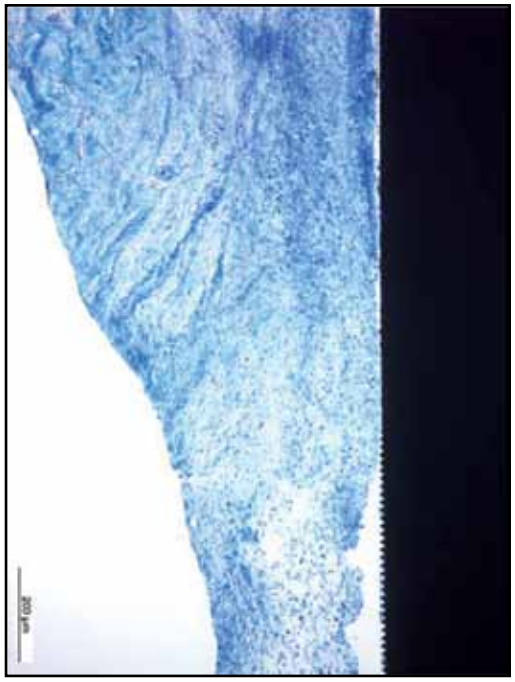

The retrieved specimen demonstrated normal peri-abutment soft tissues, without evidence of an inflammatory cell infiltrate. Polarized light imagery of mesial and distal surfaces revealed dense, obliquely oriented connective tissue fibers attaching directly to the laser microgrooved abutment surfaces.

ABSTRACT

This report presents human evidence of reattachment of the connective tissue when the laser microgrooved healing abutment has been replaced by the laser microgrooved cylindric permanent abutment. No additional bone loss has been noted 15 weeks after the placement of the laser microgrooved cylindric permanent abutment. A dense connective tissue was in intimate contact with the laser microgrooved surface to the point of the soft tissue separation, and a clear evidence of the junctional epithelium ending at the coronal-most position of the laser microgrooved zone was identified.

Clinical Evaluation of Laser Microtexturing for Soft Tissue and Bone Attachment to Dental Implants

GE Pecora, R Ceccarelli, M. Bonelli, H. Alexander, JL Ricci.

Best Clinical Innovations Presentation Award. Academy of Osseointegration 2004 Annual Meeting. Implant Dentistry. Volume 18(1). February 2009. pp. 57-66.

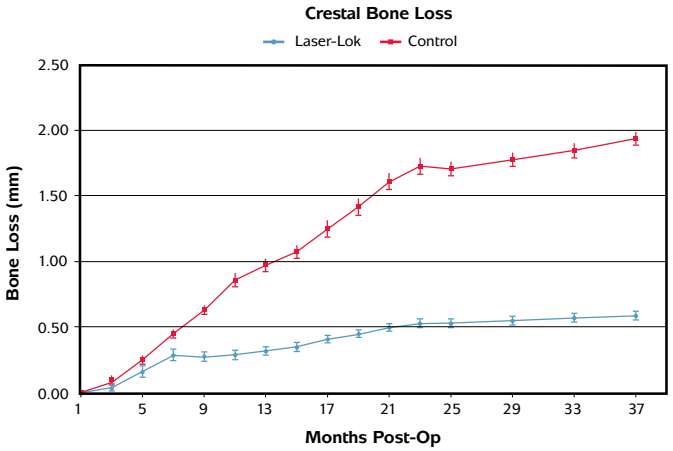

Crestal bone loss, Laser-Lok vs. Control for 37 month follow-up. Error bars=standard error; p<0.005 after month 5.

INTRODUCTION

A tapered dental implant (Laser-Lok [LL] surface treatment) with a 2 mm wide collar, that has been laser micromachined in the lower 1.5 mm to preferentially accomplish bone and connective tissue attachment while inhibiting epithelial downgrowth, was evaluated in a prospective, controlled, multicenter clinical trial.

MATERIALS

Data are reported at measurement periods from 1 to 37 months postoperative for 20 pairs of implants in 15 patients. The implants are placed adjacent to machined collar control implants of the same design. Measurement values are reported for bleeding index, plaque index, probing depth, and crestal bone loss.

RESULTS

No statistical differences are measured for either bleeding or plaque index. At all measurement periods there are significant differences in the probing depths and the crestal bone loss differences are significant after 7 months (P<0.001). At 37 months the mean probing depth is 2.30 mm and the mean crestal bone loss is 0.59 mm for LL versus 3.60 and 1.94 mm, respectively, for control implant. Also, comparing results in the mandible versus those in the maxilla demonstrates a bigger difference (control implant - LL) in the mean in crestal bone loss and probing depth in the maxilla. However, this result was not statistically significant.

DISCUSSION

The consistent difference in probing depth between LL and control implant demonstrates the formation of a stable soft-tissue seal above the crestal bone. LL limited the crestal bone loss to the 0.59 mm range as opposed to the 1.94 mm crestal bone loss reported for control implant. The LL implant was found to be comparable with the control implant in safety endpoints plaque index and sulcular bleeding index. There is a nonstatistically significant suggestion that the LL crestal bone retention superiority is greater in the maxilla than the mandible.

7 year follow-up

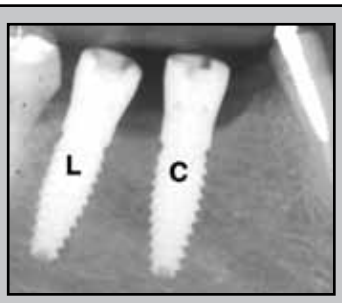

Laser-Lok (LL) and non Laser-Lok (C) at time of placement

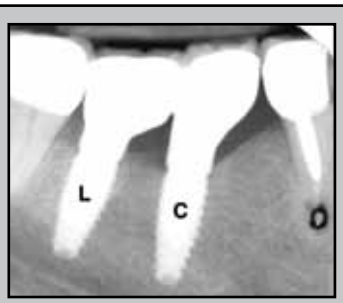

Laser-Lok (LL) and non Laser-Lok (C) at 7 years post-op

The Effects of Laser Microtexturing of the Dental Implant Collar on Crestal Bone Levels and Peri-implant Health

S Botos, H Yousef, B Zweig, R Flinton, S Weiner.

Int J Oral Maxillofac Implants 2011;26:492-498.

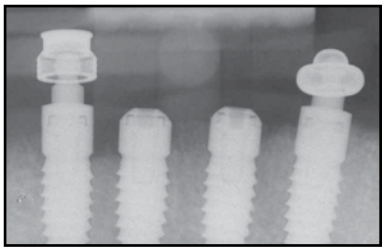

Implant placement protocol with two implants loaded and two implants unloaded.

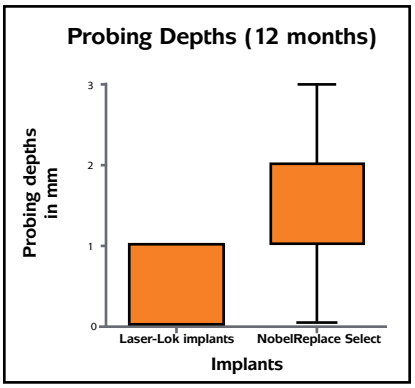

At 12-months, the Laser-Lok implants had a mean probing depth of 0.43mm versus 1.64mm for NobelReplace Select ($p <= 0.001$).

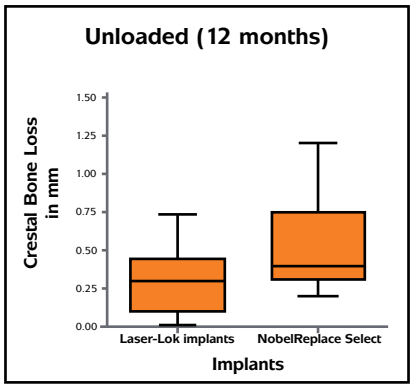

Average crestal bone loss of unloaded Laser-Lok implants was 0.29mm versus 0.55mm for NobelReplace Select ($p <= 0.01$).

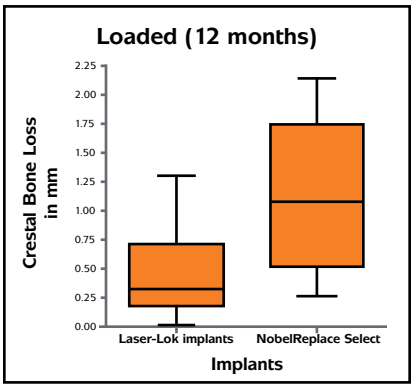

Average crestal bone loss of loaded Laser-Lok implants was 0.42mm versus 1.13mm for NobelReplace Select ($p <= 0.001$).

ABSTRACT

Purpose: Polished and machined collars have been advocated for dental implants to reduce plaque accumulation and crestal bone loss. More recent research has suggested that a roughened titanium surface promotes osseointegration and connective tissue attachment. The purpose of this research was to compare crestal bone height adjacent to implants with laser-microtextured and machined collars from two different implant systems (Laser-Lok and Nobel Replace Select).

Materials and Methods: Four implants, two Laser-Lok and two Nobel Replace Select, were placed in the anterior mandible to serve as overdenture abutments. They were placed in alternating order, and the distal implants were loaded with ball abutments. The mesial implants were left unloaded. The distal implants were immediately loaded with prefabricated dentures. Plaque Index, Bleeding Index, and probing depths (PDs) were measured after 6 and 12 months for the loaded implants. Bone loss for both groups (loaded and unloaded) was evaluated via standardized radiographs.

Results: Plaque and bleeding values were similar for both implant types. The Laser-Lok implants showed shallower PDs (0.36 ± 0.5 mm and 0.43 ± 0.51 mm) than those Nobel Replace Select (1.14 ± 0.77 mm and 1.64 ± 0.93 mm; $P < .05$ for 6 and 12 months, respectively). At 6 and 12 months, respectively, the Laser-Lok implants showed less crestal bone loss for both loaded (0.19 ± 0.15 mm and 0.42 ± 0.34 mm) and unloaded groups (0.15 ± 0.15 mm and 0.29 ± 0.20 mm) than the Nobel Replace Select implants for both the loaded (0.72 ± 0.5 mm and 1.13 ± 0.61 mm) and unloaded groups (0.29 ± 0.28 mm and 0.55 ± 0.32 mm).

Conclusion: Laser-Lok implants resulted in shallower PDs and less peri-implant crestal bone loss than that seen around Nobel Replace Select.

Case Study

Long-term case studies using a Laser-Lok implant

Courtesy of Cary Shapoff, DDS (Fairfield, CT)
Restorations by Jeffrey A. Babushkin, DDS (Trumbull, CT)

ABSTRACT

Numerous published animal and human dental implant studies report crestal bone loss from the time of placement of the healing abutment to various time periods after restoration. The bone loss can result in loss of interproximal papilla and recession of crown margins. These two case reports demonstrate the long-term results that can be obtained utilizing implants with the Laser-Lok microchannel collar design to preserve crestal bone and soft tissue esthetics. Case 1 involved extraction, socket grafting, 6 month delayed implant placement and final restoration in 6 months. Case 2 involved extraction, immediate implant placement with simultaneous grafting and provisional crown placement two months later.

Case 1

Tooth #9 prior to extraction

Bone defect immediately following extraction

A 34 year old female presented with external resorption at the level of the CEJ of tooth #9. Various treatment options were presented and the patient elected extraction and dental implant placement. After atraumatic extraction, the socket anatomy did not allow for immediate placement with acceptable initial stability. The socket was grafted with allograft calcified bone and allowed to heal for 6 months. At that time a dental implant with Laser-Lok microchannel collar design was placed. A subepithelial connective tissue graft was also utilized on the adjacent tooth #10 for root coverage. Six months after placement second stage surgery was performed and the tooth was restored with a customized abutment and PFM crown. Note the maintenance of excellent crestal bone levels (within 0.5mm of the implant/abutment interface) at 10 years post-restoration. The soft tissue margins have remained stable and exhibit excellent periodontal health.

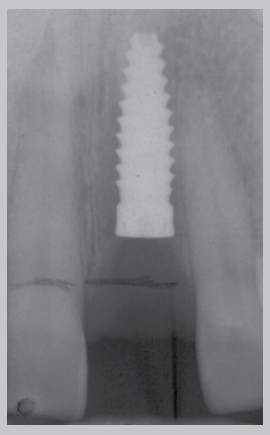

Laser-Lok implant at time of placement

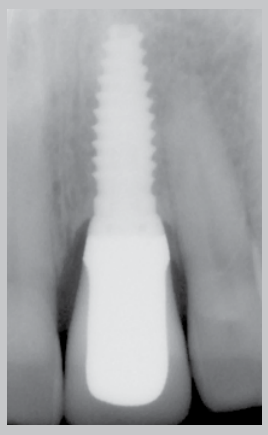

Bone levels maintained at 10 years post-restoration

Laser-Lok implant at 8 years post-restoration

Case 2

Tooth #9 with chronic infection

Tooth #9 extracted showing clinical defect

Laser-Lok implant at time of placement

Bone levels at 4 years post-restoration

Esthetics at 4 years post-restoration

This 60 year old female presented with chronic infection evidenced by a fistula at the apical extent of tooth #9. This tooth had previously been treated with root canal and apical surgery. All treatment options were reviewed with the patient and dental implant replacement was chosen. Because the patient was relocating to South America for a period of two years, immediate extraction, dental implant placement with socket grafting was performed. The dental implant was a 5 mm x 13 mm Laser-Lok microchannel collar design. A provisional crown was placed 2 months following implant placement. The patient had no other professional dental care for two years and upon returning home, the final crown was placed. Note the crestal bone levels (within 0.5 mm of the abutment/implant interface) at fours years after implant loading.

CONCLUSION

These two cases demonstrate the ability of the Laser-Lok microchannel collar design to maintain crestal bone levels and soft tissue esthetics around dental implants. Both cases involved implant placement in grafted sites. Both cases demonstrate unequivocal clinical and radiographic evidence of crestal bone stability in close proximity to the abutment/implant interface (micro-gap). A traditional expectation of bone loss below the collar and to the first thread was not noted. The ability of the Laser-Lok microchannels to maintain crestal bone and provide supracrestal connective tissue attachment may create a new definition of “normal” implant biologic width.

THE INTERNATIONAL JOURNAL OF PERIODONTICS RESTORATIVE DENTISTRY

Radiographic Analysis of Crestal Bone Levels Around Laser-Lok Collar Dental Implants

CA Shapoff, B Lahey, PA Wasserlauf, DM Kim.

Int J Periodontics Restorative Dent 2010;30:129-137

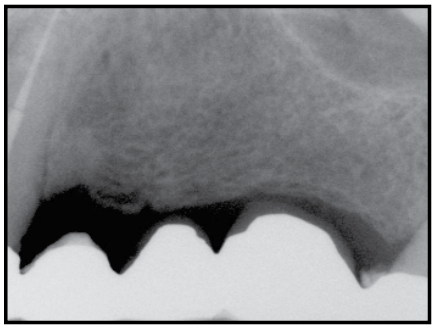

Failed bridge prior to implant placement. 4-5mm ridge required ridge splitting at implant placement.

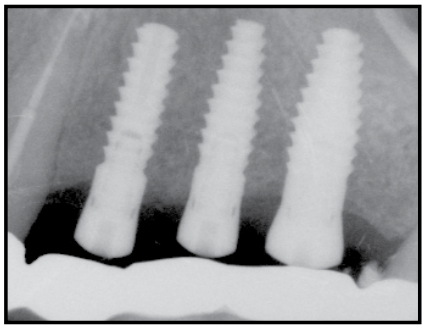

Healing abutments placed at 3.5 months. Crestal bone adjacent to Laser-Lok collar.

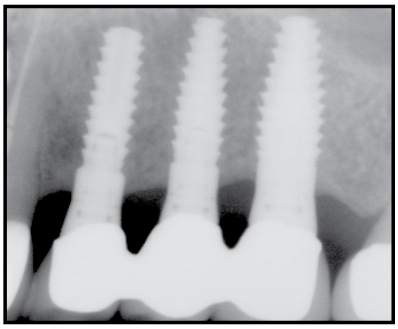

At three years, stable crestal bone adjacent to Laser-Lok collar with no indication of bone loss to the first thread.

INTRODUCTION

This retrospective radiographic study was organized to evaluate the clinical efficacy of implants with Laser-Lok microtexturing (8- and 12-µm grooves). A physical attachment of connective tissue fibers to the Laser-Lok microtexturing on the implant collar has been previously demonstrated using human histology, polarized light microscopy, and scanning electron microscopy. This analysis of 49 implants demonstrated a mean crestal bone loss of 0.44 mm at 2 years postrestoration and 0.46 mm at 3 years. All bone loss was contained within the height of the collar, and no bone loss was evident to the level of the implant threads. The radiographic evaluation of the clinical application of this implant supports previous findings that establishing a biologic seal of connective tissue fibers around a dental implant may be clinically relevant.

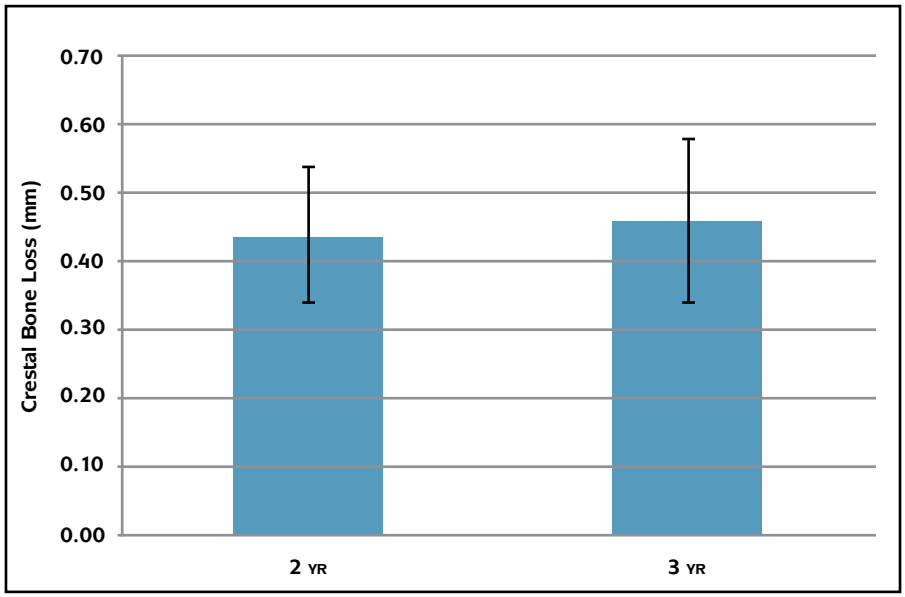

This analysis of 49 implants demonstrated a mean crestal bone loss of 0.44 mm at 2 years postrestoration and 0.46 mm at 3 years.

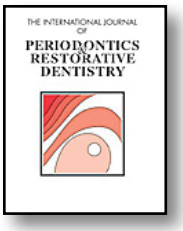

Human Histologic Evidence of a Connective Tissue Attachment to a Dental Implant

M Nevins, ML Nevins, M Camelo, JL Boyesen, DM Kim.

The International Journal of Periodontics & Restorative Dentistry. Volume 28, Number 2, 2008.

ABSTRACT

This human proof-of-principle study was designed to investigate the possibility of achieving a physical connective tissue attachment to the Laser-Lok microchannel collar of a dental implant. Its 2-mm collar has been micromachined to encourage bone and connective tissue attachment while preventing apical migration of the epithelium. Implants were harvested with the surrounding implant soft and hard tissues after 6 months. The histologic investigation was conducted with light microscopy, polarized light, and scanning electron microscopy.

RESULTS

The implants were osseointegrated with histologic evidence of direct bone contact. There was a connective tissue attachment to the Laser-Lok microchannels. There were no signs of inflammation. The peri-implant tissues consisted of a dense, collagenous lamina propria covered with a stratified, squamous, keratinizing oral epithelium. The latter was continuous with the parakeratinized sulcular epithelium that lined that lateral surface of the peri-implant sulcus. Apically, the sulcular epithelium overlapped the coronal border of the junctional epithelium. The sulcular epithelium was continuous with the junctional epithelium, which provided epithelial union between the implant and the surrounding peri-implant mucosa. Between the apical termination of the junctional epithelium and the alveolar bone crest, connective tissue directly apposed the implant surface.

Light microscopic evaluation of these specimens revealed intimate contact of the junctional epithelial cells with the implant surface. The microgrooved area of the implants was covered with connective tissue. Polarized light microscopy of this area revealed functionally oriented collagen fibers running toward the grooves of the implant surface. SEM of a corresponding area of the specimen confirmed the presence of attached collagen fibers.

All specimens demonstrated a high degree of bone-to-implant contact and intense remodeling activity. In specimens that showed collagen fibers functionally oriented toward the grooves on the implant surface, remodeling of new bone in the coronal direction was observed. SEM revealed sulcular epithelium with the desquamating activity of the cells and the junctional epithelium. It appears that the connective tissue attachment is instrumental in preserving the alveolar bone crest and inhibiting apical migration of the epithelium.

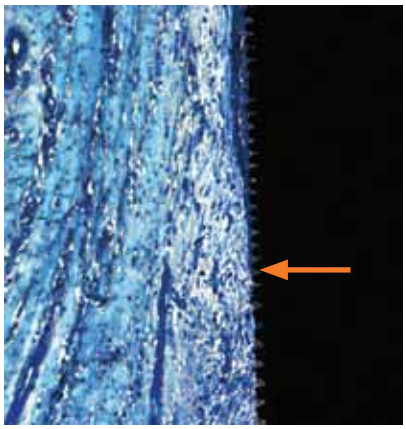

High magnification identifies the apical extent of the junctional epithelium. There is then a connective tissue attachment to the laser microchannel surface that extends to the point of bone attachment.

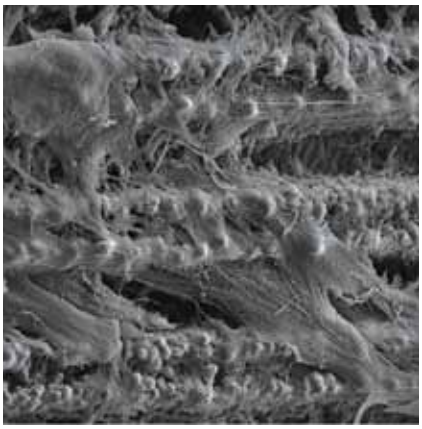

SEM showing collagen fibers attached to the rough implant surface.

Micro CT image showing an overview of osseointegration and the bone-to-implant contact (in red). Note that the level of bone contact extends to cover all threads of the implant and corresponds to the histologic observations. This supports the value of the connective tissue attachment to prevent loss of crestal bone.

Hard and Soft Tissue Changes After Crestal and Subcrestal Immediate Implant Placement

RU Koh, TJ Oh, I Rudek, GF Neiva, CE Misch, ED Rothman, HL Wang

J Periodontol 2011;82:1112-1120.

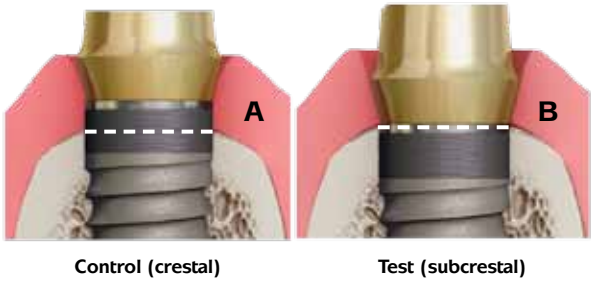

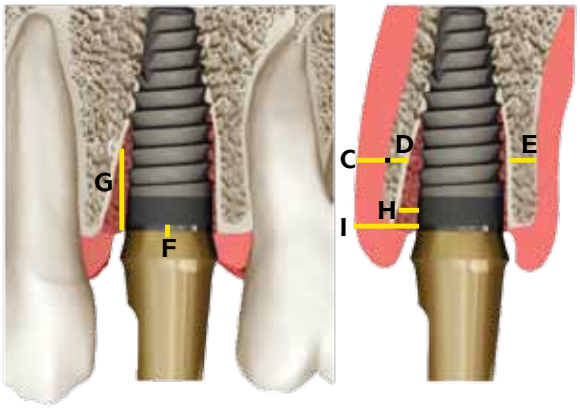

Placement level and clinical measurements. A) Crestal placement. B) Subcrestal placement. C) Facial tissue thickness. D) Facial plate thickness. E) Palatal plate thickness. F) MBL. G) TE. H) HDD. I) T-I.

BACKGROUND

The purpose of this study is to assess the influence of the placement level of implants with a laser-microtextured collar design on the outcomes of crestal bone and soft tissue levels. In addition, we assessed the vertical and horizontal defect fill and identified factors that influenced clinical outcomes of immediate implant placement.

METHODS

Twenty-four patients, each with a hopeless tooth (anterior or premolar region), were recruited to receive dental implants. Patients were randomly assigned to have the implant placed at the palatal crest or 1mm subcrestally. Clinical parameters including the keratinized gingival (KG) width, KG thickness, horizontal defect depth (HDD), facial and interproximal marginal bone levels (MBLs), facial threads exposed, tissue–implant horizontal distance, gingival index (GI), and plaque index (PI) were assessed at baseline and 4 months after surgery. In addition, soft tissue profile measurements including the papilla index, papilla height (PH), and gingival level (GL) were assessed after crown placement at 6 and 12 months post-surgery.

RESULTS

The overall 4-month implant success rate was 95.8% (one implant failed). A total of 20 of 24 patients completed the study. At baseline, there were no significant differences between crestal and subcrestal groups in all clinical parameters except for the facial MBL (P = 0.035). At 4 months, the subcrestal group had significantly more tissue thickness gain (keratinized tissue) than the crestal group compared to baseline. Other clinical parameters (papilla index, PH, GL, PI, and GI) showed no significant differences between groups at any time. A facial plate thickness <=1.5 mm and HDD >=2 mm were strongly correlated with the facial marginal bone loss. A facial plate thickness <=2 mm and HDD >=3 were strongly correlated with horizontal dimensional changes.

CONCLUSIONS

The use of immediate implants was a predictable surgical approach (96% survival rate), and the level of placement did not influence horizontal and vertical bone and soft tissue changes. This study suggests that a thick facial plate, small gaps, and premolar sites were more favorable for successful implant clinical outcomes in immediate implant placement.

Histologic Evaluation of 3 Retrieved Immediately Loaded Implants After a 4-Month Period

I Giovanna, G Pecora, A Scarano, V Perrotti, A Piattelli.
Implant Dentistry. Vol 15, Number 3, 2006.

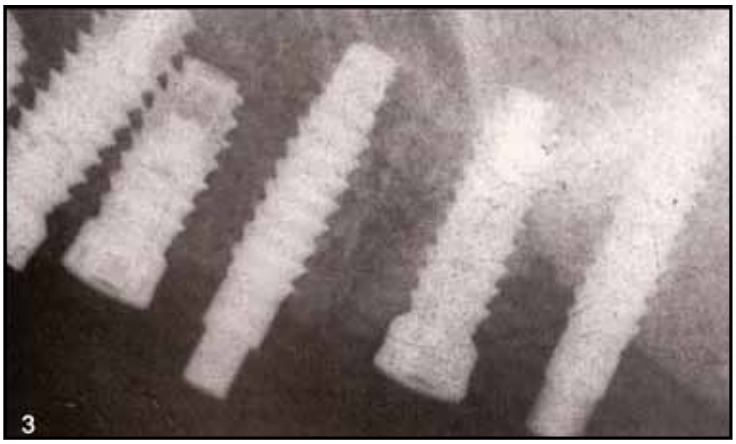

Figure 3. The definitive and provisional implants have been inserted.

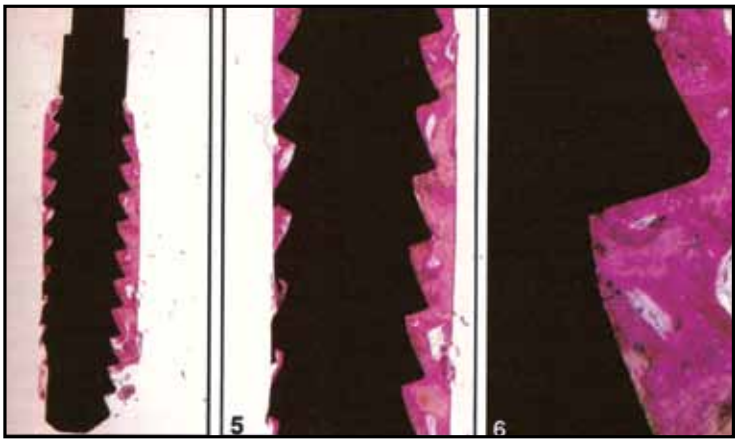

Figure 4. At low power magnification, it is possible to see that mainly lamellar bone is in contact with the implant surface. Few marrow spaces are present. The first bone to implant contact is above the level of the first thread. No areas of resorption are present at the tip of the threads (acid fushin and toluidine blue, original magnification x12).

ABSTRACT

Objective: To perform a histologic and histomorphometric analysis of the peri-implant tissue reactions and bone-titanium interface in 3 immediately loaded (provisional loaded) titanium implants retrieved from a man after a loading period of 4 months.

Materials & Methods: A 35 year-old patient with a maxillary partial edentulism did not want to wear a provisional removable prosthesis during the healing period. It was decided to insert 3 definitive implants and use 3 provisional implants for the transitional period. The provisional implants were loaded the same day with a resin prosthesis in occlusal contact. During the second surgical phase, after 4 months, the provisional prosthesis was removed, and the provisional implants were retrieved with a trephine bur. Before retrieval, all implants appeared to be clinically osseointegrated. The specimens were processed for observation under light microscopy.

Results: At low magnification, it was possible to observe that bone trabeculae were present around the implant. Areas of bone remodeling and haversian systems were present near the implant surface. Under polarized-light microscopy, it was possible to observe that in the coronal aspect of the thread, the lamellar bone showed lamellae that tended to run parallel to the implant surface, while in the inferior aspect of the thread, the bone lamellae ran perpendicular to the implant surface.

Histologic evaluation of a provisional implant retrieved from man 7 months after placement in a sinus augmented with calcium sulphate: a case report

G Iezzi, E Fiera, A Scarano, G Pecora, A Piattelli.

Journal of Oral Implantology. Volume 33, No. 2. 2007.

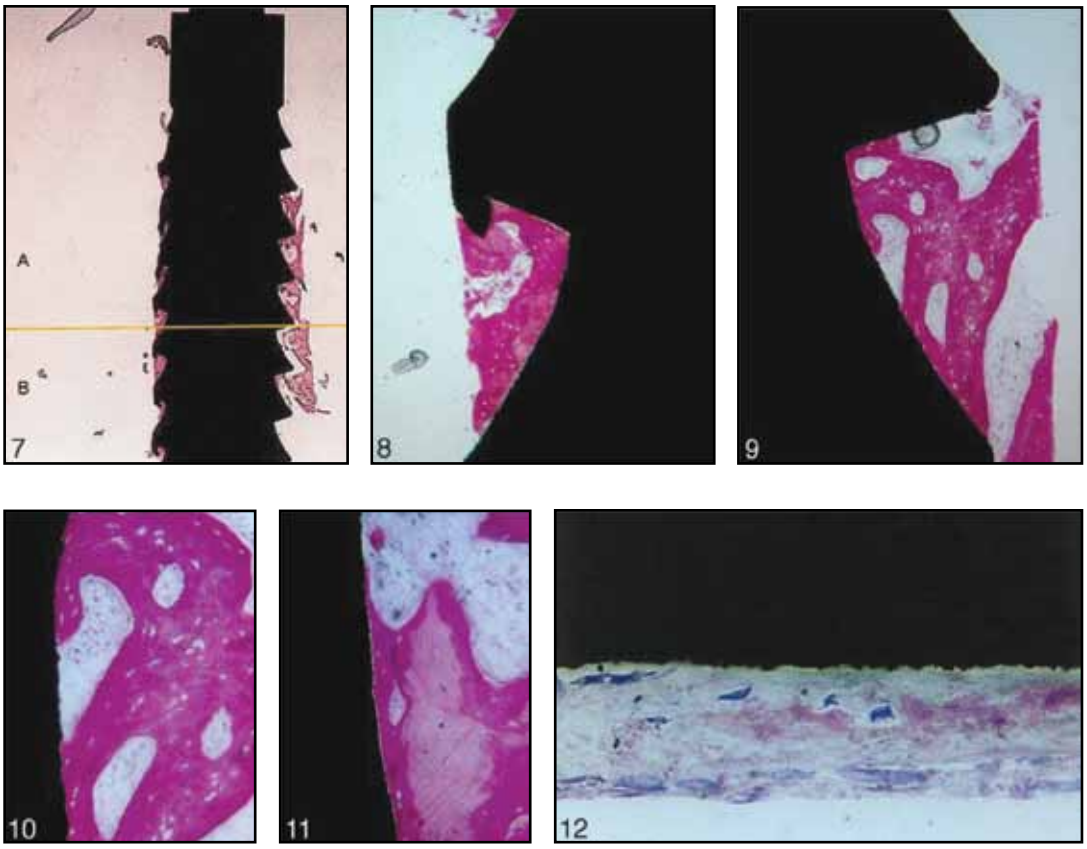

Figures 7–12. Figure 7. At low-power magnification, it is possible to see that bone is present around and in contact with the implant. The line divides native bone from newly formed bone (A) Native bone. (B) Newly formed bone. (Acid fuchsin and toluidine blue, magnification X12). FIGURE 8. Higher magnification of Figure 7 (area A). Newly formed trabecular bone with large osteocyte lacunae was present close to the implant surface. No residual calcium sulphate is present. (Acid fuchsin and toluidine blue, magnification X50). FIGURE 9. Higher magnification of Figure 7 (area A). Cortical mature bone is present near the implant surface, and bone undergoing remodeling is in direct contact with the implant surface. (Acid fuchsin and toluidine blue, magnification X100). FIGURE 10. Higher magnification of Figure 7 (area B). High magnification of the coronal portion of the bone–implant interface. Active osteoblasts secreting osteoid matrix are present. No biomaterial is present. (Acid fuchsin and toluidine blue, magnification X100). FIGURE 11. Higher magnification of Figure 7 (area B). Newly formed bone in close contact with the implant surface. Wide marrow spaces are present. No calcium sulphate is present. (Acid fuchsin and toluidine blue, magnification X50). FIGURE 12. Higher magnification of Figure 7 (area B). Osteoblasts (arrows) secreting osteoid matrix are observed in the apical portion of the implant. (Acid fuchsin and toluidine blue, magnification X400).

ABSTRACT

Little is known about the *in vivo* healing processes at the interface of implants placed in different grafting materials. For optimal sinus augmentation, a bone graft substitute that can regenerate high-quality bone and enable the osseointegration of load-bearing titanium implants is needed in clinical practice. Calcium sulphate (CaS) is one of the oldest biomaterials used in medicine, but few studies have addressed its use as a sinus augmentation material in conjunction with simultaneous implant placement. The aim of the present study was to histologically evaluate an immediately loaded provisional implant retrieved 7 months after simultaneous placement in a human sinus grafted with CaS. During retrieval, bone detached partially from one of the implants which precluded its use for histologic analysis. The second implant was completely surrounded by native and newly formed bone, and it underwent histologic evaluation. Lamellar bone, with small osteocyte lacunae, was present and in contact with the implant surface. No gaps, epithelial cells, or connective tissues were present at the bone–implant interface. No residual CaS was present. Bone–implant contact percentage was 55% ± 8%. Of this percentage, 40% was represented by native bone and 15% by newly formed bone. CaS showed complete resorption and new bone formation in the maxillary sinus; this bone was found to be in close contact with the implant surface after immediate loading.

Immediate Implant Placement and Provisionalization—Two Case Reports

SJ Froum, SC Cho, H Francisco, YS Park, N Elian, D Tarnow.
Pract Proced Aesthet Dent 2007;19(10):421-428.

Figure 1. Preoperative appearance of the FPD from the right canine to the right central incisor replacing the missing lateral incisor.

Figure 2A. Radiographic appearance of the implants immediately following placement.

Figure 3. Postoperative appearance 2.5 years following implant placement demonstrates aesthetic maintenance of the buccogingival marginal levels.

Figure 2B. Postoperative appearance 2.5 years following implant loading. Note the maintenance of the interproximal bone levels.

ABSTRACT

Endosseous dental implants have traditionally been placed using a two-stage surgical procedure with a 6- to 12-month healing period following tooth extraction. In order to decrease healing time, protocols were introduced that included immediate implant placement and provisionalization following tooth extraction. Although survival rates for this technique are high, postoperative gingival shrinkage and bone resorption in the aesthetic zone are potential limitations. The two case reports described herein present a surgical technique for the preservation of anterior aesthetics that combines minimally invasive extraction, immediate implant placement, provisionalization, and the use of implants with a laser micro-grooved coronal design.

DISCUSSION

The use of implants with a laser microgrooved coronal design may have contributed to the maintenance of buccal soft tissue, providing attachment and preventing epithelial cell downgrowth, which often occurs with machined collar implants. Maintenance of this supra crestal soft tissue often depends on its ability to establish an attachment supercrestally to the implant surface.

Influence of a microgrooved collar design on soft and hard tissue healing of immediate implantation in fresh extraction sites in dogs

SY Shin, DH Han

Clin. Oral Impl. Res. 21, 2010; 804–814.

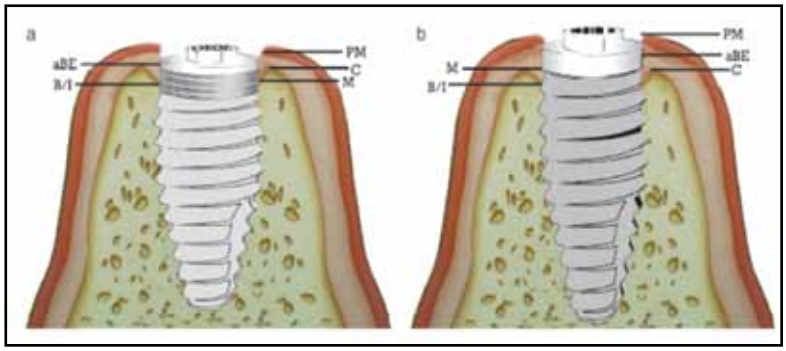

Fig. 1. Schematic drawing describing the different landmarks between which histometric measurements were performed. (a) Microgrooved collar implant group; (b) turned collar implant group. aBE, apical termination of the barrier epithelium; B/I, marginal level of bone-to-implant contact; C, marginal level of the bone crest; PM, margin of the peri implant mucosa; M, marginal level of the microgrooved surface or machined surface of implant.

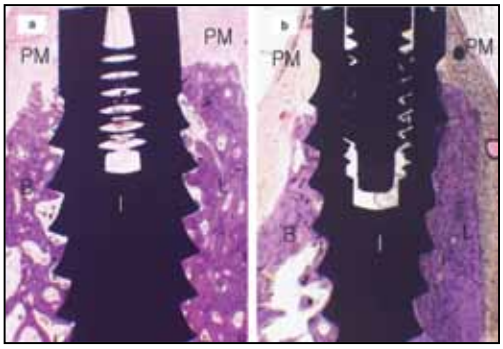

Fig. 2. Micrographs showing longitudinal section of microgrooved groups (a) and turned surface groups (b) after 12 weeks of healing. B, buccal wall; L, lingual wall; I, implant; PM, peri-implant mucosa. H-E staining; original magnification x 10.

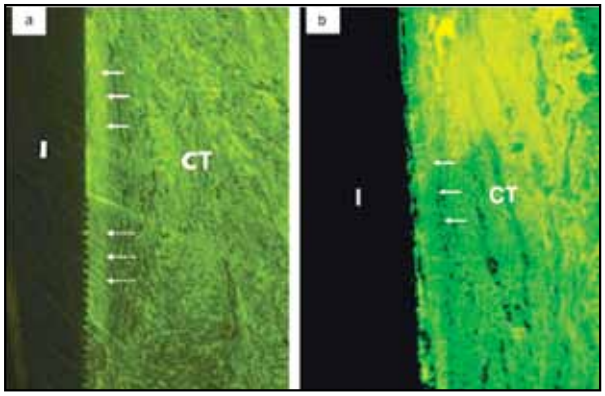

Fig. 3. Fluorescent images under polarizing microscope showing longitudinal section of microgrooved group (a) and turned surface group (b) after 12 weeks of healing. The solid arrows indicate the collagen fiber direction which are parallel to the implant surface over the turned surface and the dotted arrows point the collagen fibers perpendicular to the implant over the 8mm pitch microgrooved surface. CT, connective tissue; I, implant. Original magnification x 200.

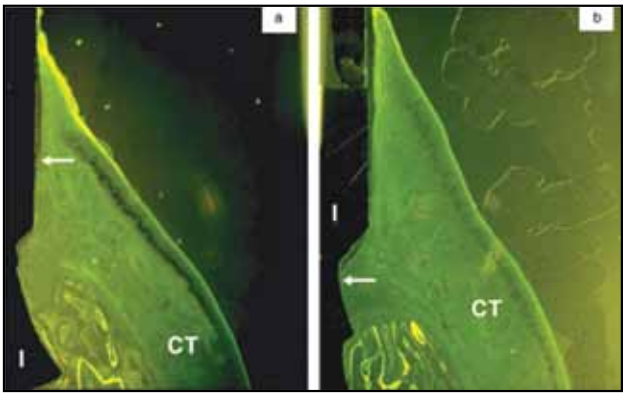

Fig. 4. Fluorescent images showing longitudinal section of microgrooved group (a) and turned surface group (b) after 12 weeks of healing. The arrows indicate the apical level of the junctional epithelium. CT, connective tissue; I, implant. Original magnification x 50.

ABSTRACT

Objective: This study compared the alveolar bone reduction after immediate implantation using microgrooved and smooth collar implants in fresh extracted sockets.

Materials and Methods: Four mongrel dogs were used in this study. The full buccal and lingual mucoperiosteal flaps were elevated and the third and fourth premolars of the mandible were removed. The implants were installed in the fresh extracted sockets. The animals were sacrificed after a 3-month healing period. The mandibles were dissected and each implant site was removed and processed for a histological examination.

Results: During healing, the marginal gaps in both groups, which were present between the implant and the socket walls at implantation, disappeared as a result of bone filling and resorption of the bone crest. The buccal bone crests were located apical of its lingual counterparts. At the 12-week interval, the mean bone–implant contact in the microgrooved collar group was significantly higher than that of the turned collar group. From the observations in some of the microgrooved collar groups, we have found bone attachment to the 12 mm microgrooved surface and collagen fibers perpendicular to the long axis of the implants over the 8 mm microgrooved surface.

Conclusion: Within the limitations of this study, microgrooved implants may provide more favorable conditions for the attachment of hard and soft tissues and reduce the level of marginal bone resorption and soft tissue recession.

Mechanical basis for bone retention around dental implants

H Alexander, JL Ricci, GJ Hrico

J Biomed Mater Res B Appl Biomater. Volume 88B, Issue 2, Pages 306-311, Feb 2009.

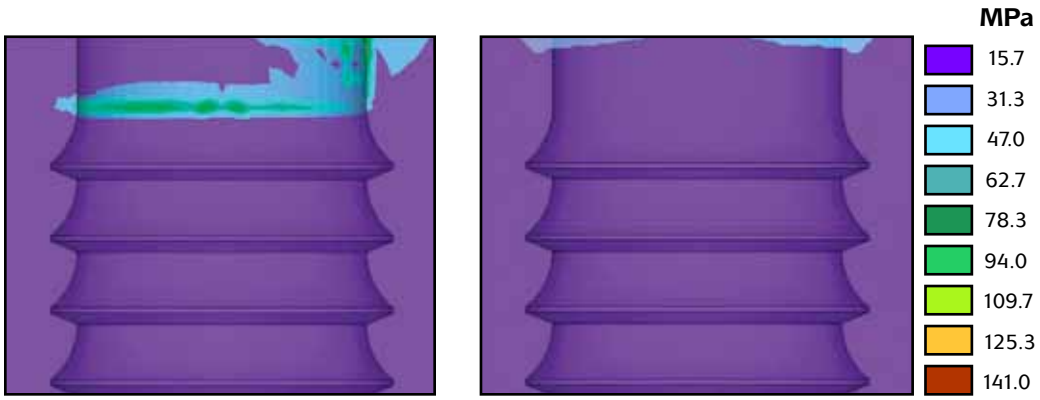

Figure 1. Max stress of 91.9 MPa seen in Control implant (left) and 22.6 MPa seen in Laser-Lok implant (right) from 80 Newton side load.

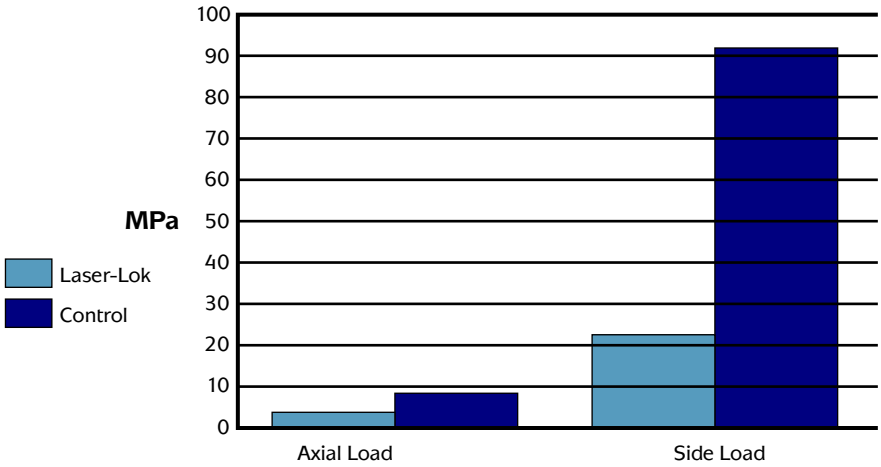

Figure 2. Summary of the results of Finite Element Analysis demonstrating the stress decrease resulting from implant attachment.

ABSTRACT

This study, analytically, through finite element analysis, predicts the minimization of crestal bone stress resulting from implant collar surface treatment. A tapered dental implant design with Laser-Lok (LL) and without (control, C) laser microgrooving surface treatment are evaluated. The LL implant has the same tapered body design and thread surface treatment as the C implant, but has a 2-mm wide collar that has been laser micromachined with 8 and 12μm grooves in the lower 1.5 mm to enhance tissue attachment. *In vivo* animal and human studies previously demonstrated decreased crestal bone loss with the LL implant. Axial and side loading with two different collar/bone interfaces (nonbonded and bonded, to simulate the C and LL surfaces, respectively) are considered. For 80 N side load, the maximum crestal bone distortional stress around C is 91.9 MPa, while the maximum crestal bone stress around LL, 22.6 MPa, is significantly lower. Finite element analysis suggests that stress overload may be responsible for the loss of crestal bone. Attaching bone to the collar with LL is predicted to diminish this effect, benefiting crestal bone retention.

Marginal Tissue Response to Different Implant Neck Design

HEK Bae, MK Chung, IH Cha and DH Han.
Yonsei University College of Dentistry, Seoul, South Korea
J Korean Acad Prosthodont. 2008 Dec;46(6):602-609.

ABSTRACT

Purpose: This animal study examined the histomorphometric variations between a turned neck (TN) implant with a RBM body, a micro-threaded (MT) neck implant and a micro-grooved (MG) implant (Laser-Lok).

Materials and Methods: Mandibular premolars from four mongrel dogs were removed and left to heal for three months. One of three different implant systems were placed according to the manufacturers' protocol and left submerged for 8 and 12 weeks. These were then harvested for histological examination. All specimens have shown uneventful healing for the duration of the experiment.

Results: The histological slides have shown that all samples osseointegrated successfully with active bone remodeling adjacent to the implants. With the Laser-Lok implants, 0.40mm and 0.26mm of marginal bone loss was observed at 8 and 12 weeks respectively. The micro-threaded implants had changes of 0.79mm and 0.56mm. The machined neck implants had marginal bone level changes of 1.61mm and 1.63mm in the 8 and 12 week specimens. A complex soft tissue arrangement was observed against micro-threaded and micro-grooved implants.

Conclusions: This is an animal study which looked at the marginal bone level and the soft tissue reaction between different implant systems with various neck designs. Within the limitation of this animal study the following statement can be concluded;

1. A clear morphometric difference in the bone area could not be noticed between MT and MG implant neck types.
2. The BIC in MG implants were slightly higher than corresponding healing times of MT and TN implants. Higher values of the BIC could be measured in week 12 specimens than in week 8 specimens.
3. In the marginal bone level, there was marked lowering with the TN implants and least with MG implants from the reference point. There were higher marginal bone levels in week 12 than week 8 in MT and MG implants specimens but with minimal differences in TN implant specimens.
4. With MT and MG implant surfaces, the collagen alignments were not parallel to the long axis of the implants. The MT and MG implants, especially MG implants had advantageous tissue response in comparison to the turned neck implants.

Table 1. Histomorphometric measurements of three different implants

Implant type Weeks	TN		MT		MG	
	8	12	8	12	8	12
BIC / %	22.28	30.49	21.78	22.56	35.51	41.02
Marginal bone loss / mm	1.61	1.63	0.79	0.56	0.4	0.26
Bone area in threads / mm	—	—	64.74	56.55	55.43	44.77

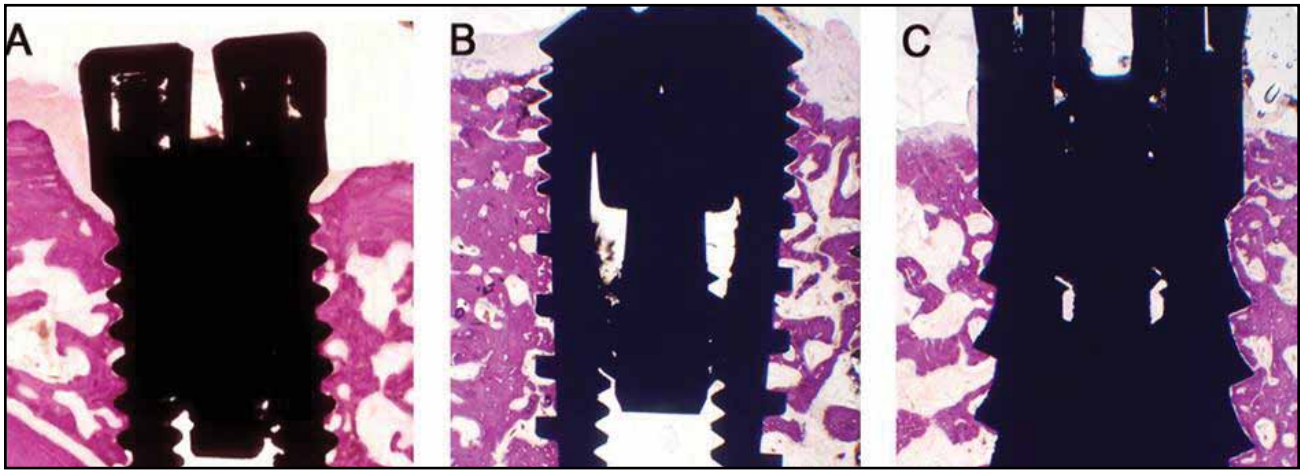

A. Turned neck implant with RBM body B. Micro-thread implant C. Laser-Lok implant

The Effects of Laser Microtextured Collars Upon Crestal Bone Levels of Dental Implants

S Weiner, J Simon, DS Ehrenberg, B Zweig, and JL Ricci.

Implant Dentistry, Volume 17, Number 2, 2008. p. 217-228.

Table 1. Nonparametric Histomorphometric Analysis Data (±Standard Error)

	Osteoclastic Activity	Saucerization	Bone Upgrowth	Soft Tissue Downgrowth
3-mo loaded specimens Control/smooth (8 sections from 3 implants)	1.50±0.29	0.92±0.05	0±0	0.83±0.10
Laser micromachined (6 sections from 4 implants)	0.88±0.16	0.50±0.10	0±0	0.25±0.13
6-mo loaded specimens Control/smooth (12 interfaces)	1.75±0.22	0.55±0.07	0.15±0.04	0.55±0.07
Laser micromachined (14 interfaces)	1.30±0.17	0.22±0.04	0.90±0.04	0±0

Fig. 1A Fig. 1B Fig. 1C

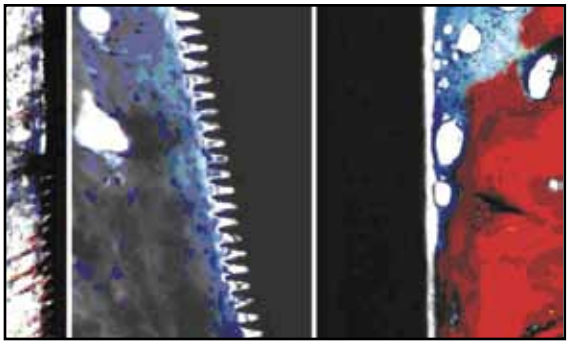

Figures 1A (left), 1B (middle), 1C (right). Light photomicrographs of epithelial and soft connective tissue interaction with experimental (1A and 1B) and control (1C) surfaces at 6 months (3 months after loading). An epithelial layer is seen in the upper portion of Fig.1A which ends in a burst of epithelial cells that are attached at the edge of the laser-micromachined region (center of photo). The lower part of Fig. 1A and all of Fig. 1B show connective attachment to the laser-micromachined surfaces. Fig. 1C shows soft tissue downgrowth between the bone and implant interface in a control implant.

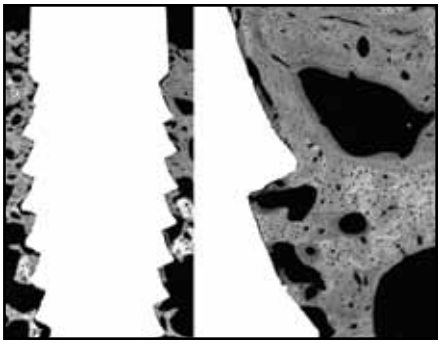

Figure 3 Scanning electron photomicrograph (backscattered electron imaging model) of bone integration of an experimental implant at 3 months (uncovering). Left: Overview (collage) of several images showing bone integration of the body of the implant as well as direct bone integration of the laser-micromachined collar. Right: Higher magnification of bone integration of the implant body. Thread pitch = 1 mm.

ABSTRACT

Purpose: The purpose of this study was to examine the crestal bone, connective tissue, and epithelial cell response to a laser microtextured collar compared with a machined collar, in the dog model.

Materials: Six mongrel dogs had mandibular premolars and first molars extracted and after healing replaced with BioLok implants 4x8 mm. Each dog had 3 control implants placed on one side of the mandible and 3 experimental, laser microtextured, implants placed contralaterally. After 3 months, 1 dog was killed. Bridges were placed on the implants of 4 of the dogs. The sixth dog served as a negative control for the duration of the experiment. Two of the dogs were killed 3 months after loading, two of the dogs were killed 6 months after loading as was the negative (unloaded) control. Histology, electron microscopy, and histomorphometric analysis was done on histologic sections obtained from block sections of the mandible containing the implants.

Results: Initially the experimental implants showed greater bone attachment along the collar. With time the bone heights along the control and experimental collars were equivalent. However, the controls had more soft tissue downgrowth, greater osteoclastic activity, and increased saucerization compared with sites adjacent to experimental implants. There was closer adaptation of the bone to the laser microtextured collars.

Conclusion: Use of tissue engineered collars with microgrooving seems to promote bone and soft tissue attachment along the collar and facilitate development of a biological width.

Connective-tissue responses to defined biomaterial surfaces. I. Growth of rat fibroblast and bone marrow cell colonies on microgrooved substrates

JL Ricci, JC Grew, H Alexander

Journal of Biomedical Materials Research Part A. 85A: 313–325, 2008.

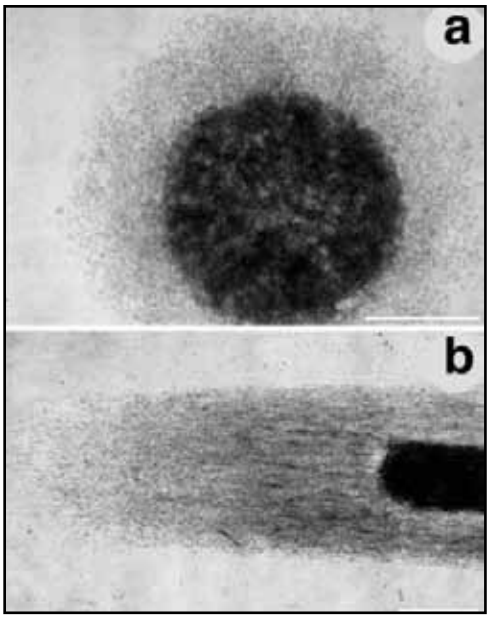

Light micrograph of RTF colonies grown for 4 days on control and 6-µm microgrooved substrates. The colony grown on the control substrate (a) displays radial outgrowth from the initial collagen gel "dot" seen as the dark area in the center of the colony. The extent of colony outgrowth can also be seen. The original gel dot is ~2 mm in diameter. The colony grown on the 6-µm microgrooved substrate (b) displays extensive outgrowth from the initial gel dot in the direction parallel with the direction of the microgrooves. Less extensive outgrowth is observed in the direction perpendicular to the direction of the microgrooves. This microgroove dimension is below the resolution limit of the microscope at this magnification. Bar = 1 mm (a and b).

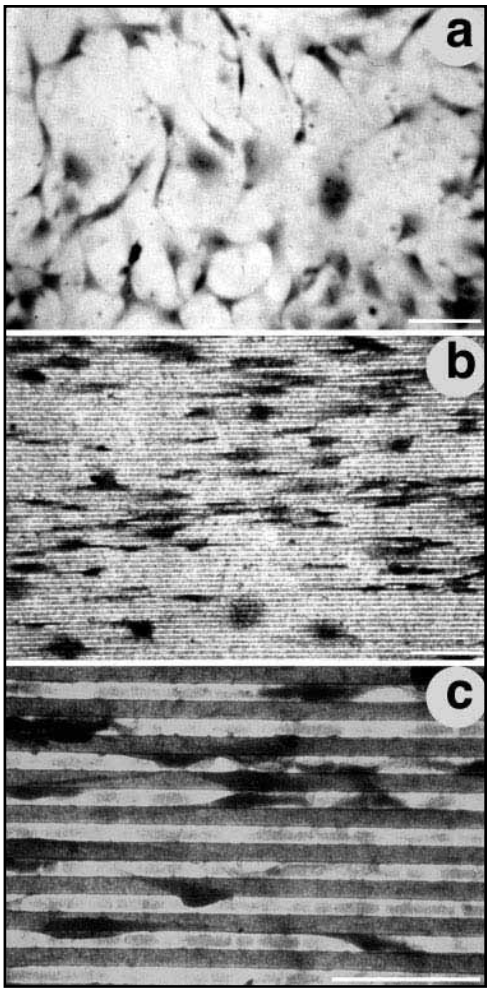

Light micrograph of RTF colonies grown for 4 days on control and 6-µm microgrooved substrates. The colony grown on the control substrate (a) displays radial outgrowth from the initial collagen gel "dot" seen as the dark area in the center of the colony. The colony grown on the 6-µm microgrooved substrate (b) displays extensive outgrowth from the initial gel dot in the direction parallel with the direction of the microgrooves. Bar = 100 µm (a and b).

ABSTRACT

Surface microgeometry plays a role in tissue implant surface interactions, but our understanding of its effects is incomplete. Substrate microgrooves strongly influence cells *in vitro*, as evidenced by contact guidance and cell alignment. We studied "dot" colonies of primary fibroblasts and bone marrow cells that were grown on titanium-coated, microgrooved polystyrene surfaces that we designed and produced. Rat tendon fibroblast and rat bone marrow colony growth and migration varied ($p < 0.01$) by microgroove dimension and slightly by cell type. We observed profoundly altered morphologies, reduced growth rates, and directional growth in colonies grown on microgrooved substrates, when compared with colonies grown on flat, control surfaces ($p < 0.01$). The cells in our colonies grown on microgrooved surfaces were well aligned and elongated in the direction parallel to the grooves and colonies. Our "dot" colony is an easily reproduced, easily measured and artificial explant model of tissue-implant interactions that better approximates *in vivo* implant responses than culturing isolated cells on biomaterials. Our results correlate well with *in vivo* studies of titanium dioxide-coated polystyrene, titanium, and titanium alloy implants with controlled microgeometries. Microgrooves and other surface features appear to directionally or spatially organize cells and matrix molecules in ways that contribute to improved stabilization and osseointegration of implants.

Connective-tissue responses to defined biomaterial surfaces. II. Behavior of rat and mouse fibroblasts cultured on microgrooved substrates

JC Grew, JL Ricci, H Alexander

Journal of Biomedical Materials Research Part A. 85A: 326-335, 2008.

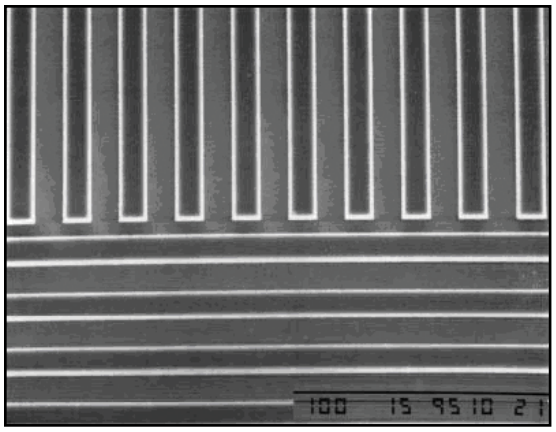

Scanning electron micrograph of a portion of a silicon-wafer mold bearing 12-µm microgrooves. Bar = 100 µm.

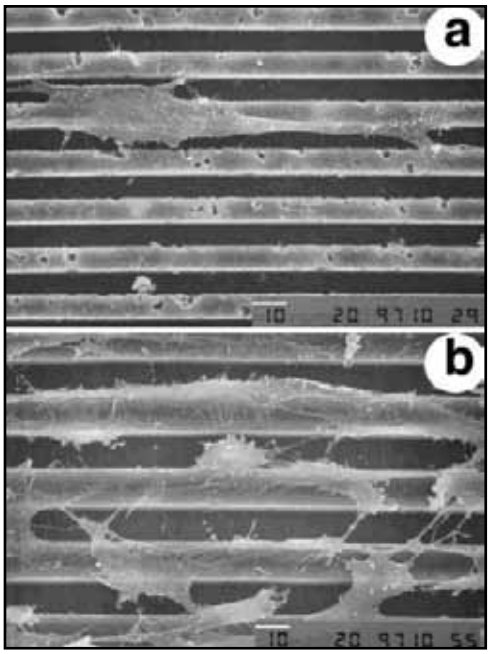

Scanning-electron micrographs of NIH-3T3 fibroblasts grown on 8- (a) and 12-µm (b) microgrooved substrates for 8 days. The individual cell grown on 8-µm grooves is attached to several adjacent ridges, bridging the intervening grooves. The cells grown on 12-µm grooves most frequently lie atop the ridges or within the grooves. Both microgroove dimensions impose a strong orientation effect upon the cells. Bar = 10 µm.

ABSTRACT

Surface microgeometry strongly influences the shapes, orientations, and growth characteristics of cultured cells, but in-depth, quantitative studies of these effects are lacking. We investigated several contact guidance effects in cells within "dot" colonies of primary fibroblasts and in cultures of a transformed fibroblast cell line, employing titanium-coated, microgrooved polystyrene surfaces that we designed and produced. The aspect ratios, orientations, densities, and attachment areas of rat tendon fibroblasts (RTF) colony cells, in most cases, varied ($p < 0.01$) by microgroove dimension. We observed profoundly altered cell morphologies, reduced attachment areas, and reduced cell densities within colonies grown on microgrooved substrates, compared with cells of colonies grown on flat, control surfaces. 3T3 fibroblasts cultured on microgrooved surfaces demonstrated similarly altered morphologies. Fluorescence microscopy revealed that microgrooves alter the distribution and assembly of cytoskeletal and attachment proteins within these cells. These findings are consistent with previous results, and taken together with the results of our *in vivo* and cell colony growth studies, enable us to propose a unified hypothesis of how microgrooves induce contact guidance.

Osseointegration on metallic implant surfaces: effects of microgeometry and growth factor treatment

SR Frenkel, J Simon, H Alexander, M Dennis, JL Ricci.

J Biomed Mater Res. 2002;63(6):706-13.

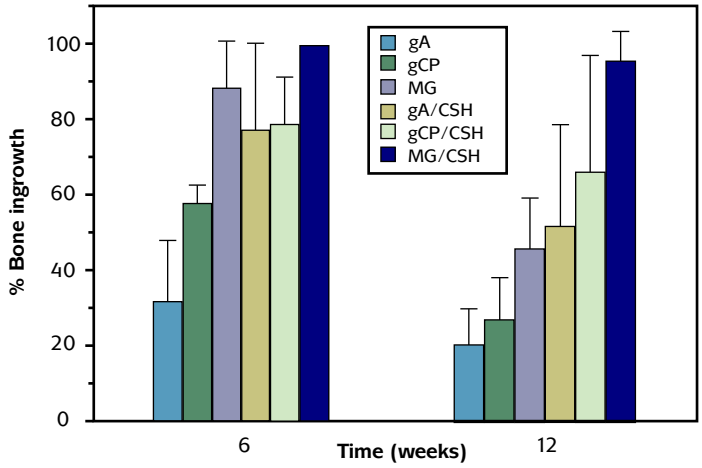

Figure 1. Percentage of bone ingrowth into channels at 6 and 12 weeks.

ABSTRACT

Orthopedic implants often loosen due to the invasion of fibrous tissue. The aim of this study was to devise a novel implant surface that would speed healing adjacent to the surface, and create a stable interface for bone integration, by using a chemoattractant for bone precursor cells, and by controlling tissue migration at implant surfaces via specific surface microgeometry design. Experimental surfaces were tested in a canine implantable chamber that simulates the intramedullary bone response around total joint implants. Titanium and alloy surfaces were prepared with specific microgeometries, designed to optimize tissue attachment and control fibrous encapsulation. TGFβ, a mitogen and chemoattractant (Hunziker EB, Rosenberg LC. J Bone Joint Surg Am 1996;78:721-733) for osteoprogenitor cells, was used to recruit progenitor cells to the implant surface and to enhance their proliferation. Calcium sulfate hemihydrate (CS) was the delivery vehicle for TGFβ; CS resorbs rapidly and appears to be osteoconductive. Animals were sacrificed at 6 and 12 weeks postoperatively. Results indicated that TGFβ can be reliably released in an active form from a calcium sulfate carrier *in vivo*. The growth factor had a significant effect on bone ingrowth into implant channels at an early time period, although this effect was not seen with higher doses at later periods. Adjustment of dosage should render TGFβ more potent at later time periods. Calcium sulfate treatment without TGFβ resulted in a significant increase in bone ingrowth throughout the 12-week time period studied. Bone response to the microgrooved surfaces was dramatic, causing greater ingrowth in 9 of the 12 experimental conditions. Microgrooves also enhanced the mechanical strength of CS-coated specimens. The grooved surface was able to control the direction of ingrowth. This surface treatment may result in a clinically valuable implant design to induce rapid ingrowth and a strong bone-implant interface, contributing to implant longevity.

Interactions between MC3T3-E1 cells and textured Ti6Al4V surfaces

Soboyejo WO, Nemetski B, Allameh S, Marcantonio N, Mercer C, Ricci J.

J Biomed Mater Res. 2002 Oct; 62(1):56-72.

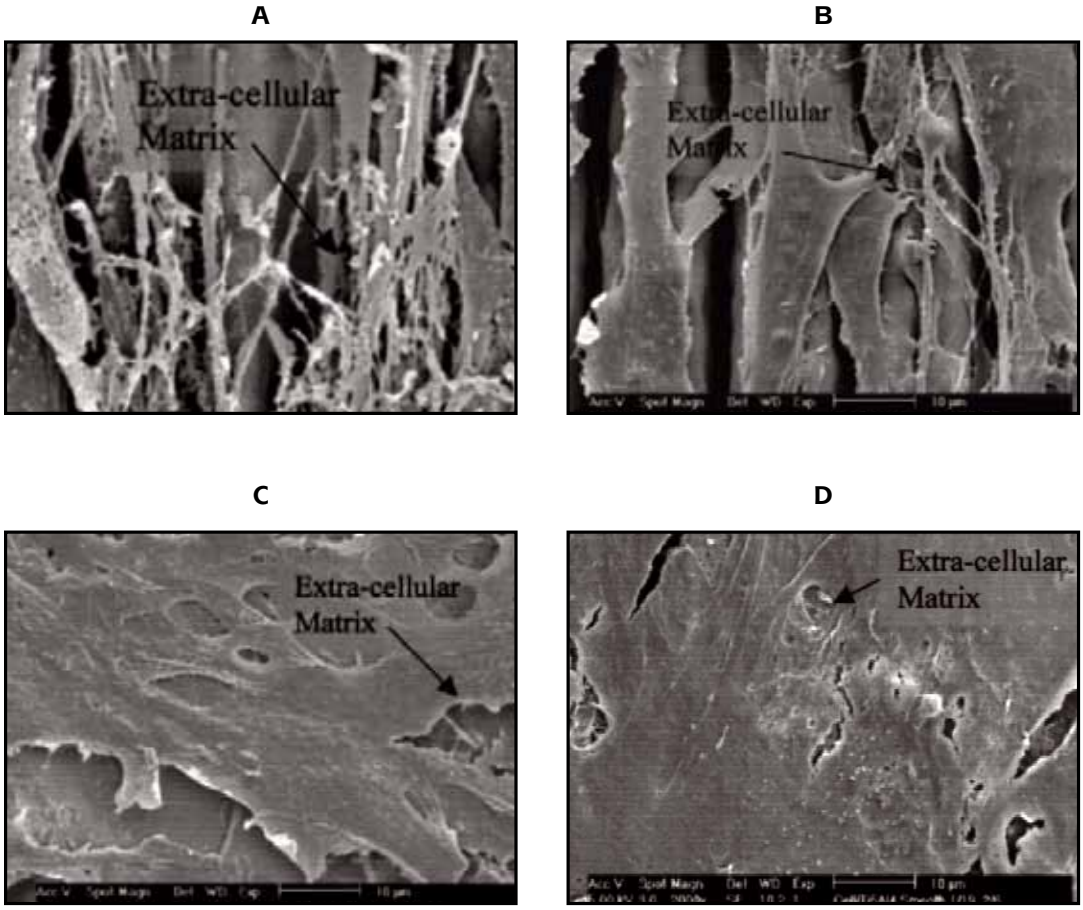

Figure 1. Extracellular matrix formation after 9 days of cell culture on (a) 12-μm microgrooved substrate; (b) 8-μm microgrooved substrate; (c) Al_2O_3-blasted surfaces; and (d) smooth surfaces.

ABSTRACT

This paper presents the results of an experimental study of the interactions between MC3T3-E1 (mouse calvarian) cells and textured Ti6Al4V surfaces, including surfaces produced by laser microgrooving; blasting with alumina particles; and polishing. The multiscale interactions between MC3T3-E1 cells and these textured surfaces are studied using a combination of optical scanning transmission electron microscopy and atomic force microscopy. The potential cytotoxic effects of microchemistry on cell-surface interactions also are considered in studies of cell spreading and orientation over 9-day periods. These studies show that cells on microgrooved Ti6Al4V geometries that are 8 or 12 micron deep undergo contact guidance and limited cell spreading. Similar contact guidance is observed on the surfaces of diamond-polished surfaces on which nanoscale grooves are formed due to the scratching that occurs during polishing. In contrast, random cell orientations are observed on alumina-blasted Ti6Al4V surfaces. The possible effects of surface topography are discussed for scar-tissue formation and improved cell-surface integration.

Tissue Response to Transcutaneous Laser Microtextured Implants

CL Ware, JL Simon, JL Ricci.

Presented at the 28th Annual Meeting of the Society for Biomaterials.
April 24-27, 2002. Tampa, FL.

Figure 1. **(A)** Scanning electron micrograph (SEM) of the surface of a laser microtextured implant. The microtexturing is in two bands on the two millimeter-wide collar. **(B)** Higher magnification SEM of the laser microtextured surface showing 12µm grooves and ridges (bar = 40µm).

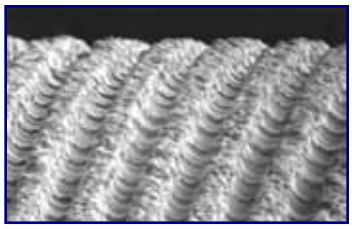

ABSTRACT

Introduction: This report describes the use of laser-microtextured transcutaneous implants in a rabbit calvarial model to enhance soft tissue integration. Dental and orthopaedic implants are routinely microtextured to enhance tissue integration. Computer-controlled laser microtexturing techniques that produce microgrooved surfaces with defined 8-12µm features on controlled regions of implant surfaces have been developed based on results from cell culture experiments and *in vivo* models. These textures have been replicated onto the collars of dental implants to provide specific areas for both osteointegration and the formation of a stable soft tissue-implant interface. The objective of this study is to evaluate these implants in a transcutaneous rabbit calvarial model to determine whether controlled laser microtexturing can be used to create a stable interface with connective tissue and epithelium.

Methods: Laser microtextures were produced on the 4mm diameter collars of modified dental implants designed for rabbit studies (Figure 1). The implants were 4.5mm in length and the threaded portion was 3.75mm in diameter. Implants were produced and supplied by Orthogen Corporation (Springfield, NJ) and BioLok International (Deerfield Beach, FL). The implant surfaces were modified by ablation of defined areas, using an Excimer laser and large-area masking techniques. Controlled laser ablation allows accurate fabrication of defined surface microstructure with resolution in the micron scale range. Laser machined surfaces contained 8µm and 12µm microgrooved systems oriented circumferentially on the collars. The collars of the control implants were "as machined", and were characterized by small machining marks on their surfaces. All implants were cleaned and passivated in nitric acid prior to sterilization.

Four transcutaneous implants were surgically implanted bilaterally in the parietal bones in each rabbit using single-stage procedures. The surgical protocol was similar to dental implant placement. An incision was made over the sagittal suture, and the skin and soft tissues were reflected laterally. Implants were placed using pilot drills and fluted spade drills to produce 3.4mm sites for the 3.75mm diameter implants. The implants were placed with the threaded portion in bone, and the laser-microtextured collar penetrating the subcutaneous soft tissue and epithelium. Each rabbit received two implants on either side of the midline (1 control and 3 experimental implants per subject). The skin was then sutured over the implants. Punch openings were made to expose the tops of the platforms of the implants, and the cover screws were used to fasten down small plastic washers coated with triple antibiotic ointment. The plastic washers were used to prevent the skin from closing over the implant during the swelling that occurred during early healing. They were removed after two weeks. Twelve rabbits were used in the study. Rabbits were sacrificed at 2, 4 and 8 weeks, and the implants and surrounding tissues were processed for histology. Hard and soft tissue response to the implants was examined histologically.

Results and Discussion: No complications or infections were encountered during the course of the experiment. The 2 and 4 week histology displayed immature soft tissue formations around all implants, and little epithelial interaction with the implant surfaces was noted as the epithelium had not regenerated at the implant surface by 2 weeks, and no clear relationship between epithelium and implant was seen at 4 weeks. 8-week samples showed more mature soft tissue and epithelial tissue. In these samples, the epithelium had fully regenerated and the soft tissue showed more mature and organized collagen. In the control samples, the epithelium consistently grew down the interface between implant and soft tissue and formed a deep sulcus along the implant collar. This sulcus extended to the bone surface and there was little or no direct soft tissue interaction or integration with the control surfaces. The 8-week laser machined implants produced a different pattern of tissue interaction. The epithelium also produced a sulcus at the upper collars of these implants. However, in most cases the sulcus did not extend down as far as the bone surface, but ended at a 300-700µm wide band of tissue, which was attached to the base of the microtextured collar. Even though the laser-microtexturing extended to the top of the collar, this soft tissue attachment formed only at the lower portion of the implant collar, where a stable "corner" of soft tissue attached to both the implant collar and the bone surface. This arrangement of sulcus, epithelial attachment, and soft tissue attachment was similar to the "biologic width" structural arrangement that has been described around teeth and in some cases around implants.

Conclusions: This preliminary study suggests that laser microtextured surfaces can be applied to transcutaneous implants and used to improve soft tissue integration. Results suggested that the soft tissues at the skin interface are capable of producing an arrangement similar to the "biologic width" arrangement seen around teeth. These laser-machined microtextures are hypothesized to work by increasing surface and organization of attached cells and tissues. They can be used to form a functionally stable interface with soft tissues, establishing an effective transcutaneous barrier. While longer-term studies are needed, the results suggest that performance of transcutaneous prosthetic fixation may be enhanced through the use of regional organized microtexturing.

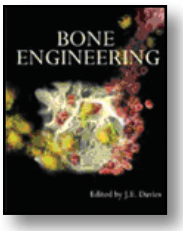

Bone Response to Laser Microtextured Surfaces

JL Ricci, J Charvet, SR Frenkel, R Change, P Nadkarni, J Turner and H Alexander.
Bone Engineering (editor: JE Davies). Chapter 25.
Published by Em2 Inc., Toronto, Canada. 2000.

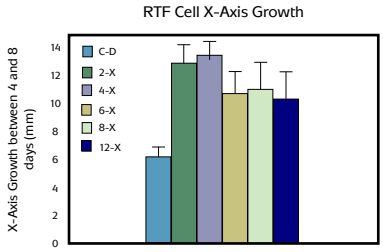

Figure 1. Graphs of X-axis growth by RTF cells on microgrooved surfaces after 8 days compared to control colonies (diameter increase).

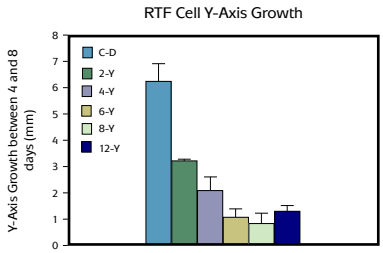

Figure 2. Graphs of Y-axis growth by RTF cells on microgrooved surfaces after 8 days compared to control colonies (diameter increase).

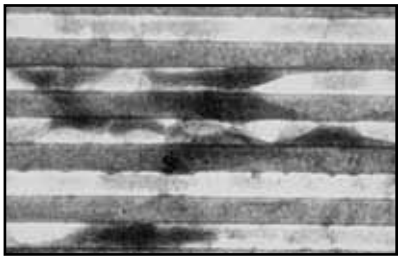

Figure 3. Light photomicrograph of RTF cells growing on a 12 µm microgrooved culture surface. Cells are attached to tops, bottoms and sides of grooves. Cells are aligned along the long axis of the substrate.

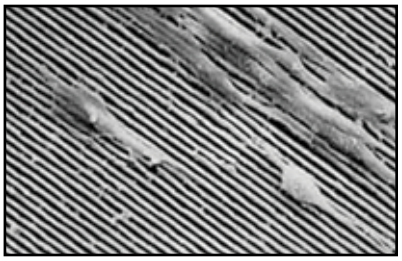

Figure 4. Scanning electron micrograph of RTF cells growing on a 2 µm microgrooved culture surface. Cells are attached to tops of grooves and span several grooves. Cells are aligned along the long axis of the substrate. Bar=100 µm.

INTRODUCTION

Tissue response to any implantable device has been found to correlate with a complex combination of material interface parameters based on composition, surface chemistry, and surface microgeometry. The relative contributions of these factors are difficult to assess.

In vitro and *in vivo* experiments have demonstrated the role of surface microgeometry in tissue-implant surface interaction although no well-defined relationship has been established. The general relationship, as demonstrated by *in vivo* experiments on metallic and ceramic implants indicates that smooth surfaces promote formation of thick fibrous tissue encapsulation and rough surfaces promote thinner soft tissue encapsulation and more intimate bone integration. Smooth and porous titanium surfaces have also been shown to have different effects on the orientation of fibrous tissue cells *in vitro*. Surface roughness has been shown to be a factor in tissue integration of implants with hydroxyapatite surfaces, and to alter cell attachment and growth on polymer surfaces roughened by hydrolytic etching. Roughened surfaces have also shown pronounced effects on differentiation and regulatory factor production of bone cells *in vitro*. Defined surface microgeometries, such as grooved and machined metals and polymer surfaces have been shown to cause cell and ECM orientation *in vivo* and can be used to encourage or impede epithelial downgrowth in experimental dental implants. Surface texturing has also been shown to adhere fibrin clot matrix more effectively than smooth surfaces, forming a more stable interface during the collagenous matrix contracture that occurs during healing. This is an effect which may be important in determining early events in tissue integration.

It is likely that textured surfaces work on several levels. These surfaces have higher surface areas than smooth surfaces and interdigitate with tissue in such a way as to create a more stable mechanical interface. They may also have significant effects on adhesion of fibrin clot, adhesion of more permanent extracellular matrix components, and long-term interaction of cells at stable interfaces. We have observed that, in the short term, fibrous tissue cells form an earlier and more organized collagenous capsule at smooth interfaces than at textured interfaces. We suggest that textured surfaces have an additional advantage over smooth surfaces. They inhibit colonization by fibroblastic cell types that arrive early in wound healing and encapsulate smooth substrates.

We have investigated (1) the effects of textured surfaces on colony formation by fibroblasts, and (2) the effects of controlled surface microgeometries on fibroblast colonization. Based on these results, we have designed, fabricated, and tested titanium alloy and commercially-pure titanium implants with controlled microgeometries in *in vivo* models. These experimental surfaces have highly-oriented, consistent microstructures which are applied using computer-controlled laser ablation techniques. The results suggest that controlled surface microgeometry, in specific size ranges, can enhance bone integration and control the local microstructural geometry of attached bone.

Cytoskeletal Organization in Three Fibroblast Variants Cultured on Micropatterned Surfaces

JC Grew, JL Ricci.

Presented at the Sixth World Biomaterials Congress. Kamuela, HI. May 15-20, 2000.

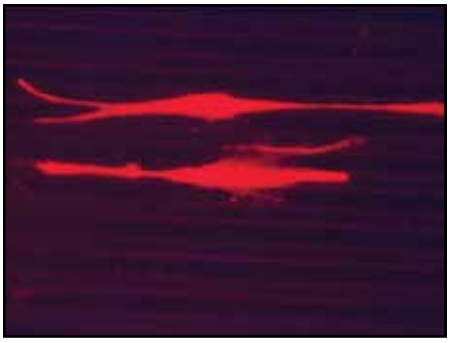

Figure 1. 3T3-L1 fibroblasts cultured on 12 µm grooves. Note the uniform orientation of the elongated cells.

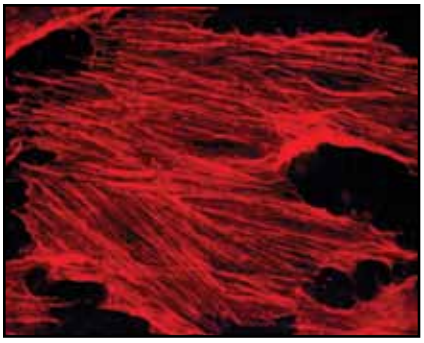

Figure 2. MC-3T3 fibroblasts cultured on a smooth surface.

ABSTRACT

Introduction: Implant surface geometry and microgeometry influence tissue responses to implants. The physical and chemical properties of synthetic substrates affect the morphology, physiology and behavior of cultured cells of various types. To date, studies of tissue-implant interaction have emphasized cell attachment, signaling and other cellular response mechanisms. Cellular attributes influenced by micrometric substrate features include cell shape, attachment, migration, orientation, and cytoskeletal organization. We studied three phenotypic variants of a murine fibroblast cell line to explore the influence of substrate microgeometry on cell shape, orientation, and microfilament distribution. Microfilament organization reflects cell shape and orientation, attendant to cell signaling events that also regulate cell attachment, mitosis, migration and apoptosis. Microfilament bundles (stress fibers) terminate at clusters of actin-associated proteins, adhesion molecules, and protein kinases which contribute to *in vitro* cell responses to culture substrates.

Methodology: NIH-3T3 fibroblasts, 3T3-Li fibroblasts (ATCC, Manassas, VA) and MC-3T3 fibroblasts (gift of JP O'Connor) were grown in DMEM with 10% NCS and 1% antibiotics in 24-well plates containing TiO_2-coated, microtextured polystyrene inserts. Culture substrates had either 8µm parallel grooves, 12µm parallel grooves, 3x3µm square posts separated by 3µm perpendicular grooves, or no features (controls). Ten thousand cells were seeded into wells containing the inserts and after 1 day, were prepared for scanning electron microscopy (SEM) or stained with rhodamine-phalloidin.

Results: All three variants of 3T3 fibroblasts adhered to all substrates within 1 day. There was no predominant orientation or shape in cells grown on control surfaces. The cytoplasms of some cells grown on control surfaces showed random arrays of stress fiber, apparently terminating at focal adhesions. Nearly all cells of all types grown on 8 or 12µm grooved substrates were elongated and oriented parallel to the grooves, growing atop the ridges or within the troughs (Figure 1). Cells cultured on 8µm grooves bridged grooves more frequently than cells cultured on 12µm grooves. Few cells of any type demonstrated evidence of stress fibers formation after 1 day in culture on grooved surfaces. Many cells grown on posted substrates displayed stress fibers terminating on posts. These assumed a stellate conformation, with process extending orthogonally from a central cytoplasmic mass and terminating atop the elevated posts (Figure 1). This finding is similar to our previous observations of NIH-3T3 cells grown on posted substrates. SEM observations confirmed the shape and orientation effects of the substrates on the 3T3 variants.

Discussion: This experiment demonstrated that parallel and intersecting grooves dictate the cell shape, orientation and cytoskeletal organization of three phenotypic variants of 3T3 fibroblasts. The NIH-3T3 variant is a fibrogenic line, while the 3T3-L1 variant is lipogenic and the MC-3T3 variant is osteogenic. The phenotypes of these cells were assessed by alkaline phosphatase assay (MC-3T3 cells are alkaline phosphatase positive) and by Sudan Black B staining (for lipid inclusions in 3T3-Li cells). The roles of extracellular matrix and cell adhesion molecules in the contact guidance events described above were not characterized, but are not discounted. We have previously demonstrated that integrin distribution and tyrosine kinase activity is physically constrained by micrometric substrate features. We hypothesize that the same constraint has occurred in the cells described herein. Elucidation of phenotypic differences between cell types that direct the tissue response to implants may yield information leading to improved implant integration and extended implant lifespan.

Acknowledgements: This work was aided by NSF grants SBIR-9160684 and DUE-9750533, and by NJCU SBR grant 220253. Microgeometry molds were prepared by the Cornell Nanofabrication Facility.

Cytological Characteristics of 3T3 Fibroblasts Cultured on Micropatterned Substrates

JC Grew, SR Frenkel, E Goldwyn, T Herman, and JL Ricci.

Presented at the 24th Annual Meeting of the Society for Biomaterials. April 22-26, 1998. San Diego, CA.

ABSTRACT

Introduction: Implant surface geometry and microgeometry affect tissue responses, although the tissue-implant interaction is incompletely characterized. Physical and chemical properties of synthetic substrates affect the morphology, physiology and behavior of cultured cells of various types. Investigators are just now beginning to describe these *in vitro* effects in detail. Shape, attachment, migration, orientation, and cytoskeletal organization differ between cells cultured on flat substrates and substrates having regular surface features of micrometric dimensions. We studied murine fibroblast shape, orientation, and microfilament and focal adhesion distribution – parameters relevant to contact guidance and to other factors influenced by substrate microgeometry. Microfilament organization reflects cell shape and orientation, but is also important in signal transduction schemes governing cell attachment, mitosis, migration and apoptosis. Microfilament bundles terminate in clusters of actin-associated proteins, adhesion proteins, and protein kinases having signal transduction functions. We employed assays that revealed the distribution of (1) microfilaments/stress fibers; (2) focal adhesion molecules; and (3) phosphotyrosine, the product of the major class of kinases associated with cell attachments.

Methodology: 3T3 fibroblasts (ATCC, Rockville, MD) from frozen stocks were grown in DMEM with 10% FBS in multiwell plates containing 1cm square microtextured inserts. The inserts consisted of polystyrene solvent cast on silicon molds and titanium-oxide coated. The resultant surfaces had either 8µm parallel grooves, 12µm parallel grooves, 3µm square posts (created by perpendicular 3µm grooves), or no features (controls). Four thousand cells were seeded into wells containing the inserts and after 4 or 8 days were prepared for scanning electron microscopy (SEM) or stained with (1) rhodamine-phalloidin; (2) either mouse antitalin or mouse antivinculin followed by rhodamine-antimouse antibodies; or (3) fluorescein-antiphosphotyrosine antibody.

Results: By day 4, the 3T3 cells had adhered to all substrates, and by day 8 they showed considerable growth in places approaching confluences. There was no predominant orientation or shape in cells grown on control surfaces. Their cytoplasms showed diffuse rhodamine staining; demonstrable stress fibers were absent. Focal adhesions and phosphotyrosine were diffusely distributed. Cells grown on 8 or 12µm grooved substrates were nearly uniformly oriented in the direction of the grooves. Cells cultured on 8µm grooves mostly grew atop the ridges, often bridging the troughs between ridges. Cells cultured on 12µm grooves mostly grew either atop the ridges or within the troughs, only infrequently bridging the troughs between ridges. Some cells demonstrated limited evidence of stress fibers after 8 days in culture on the grooved surfaces. Focal adhesions and phosphotyrosine were limited to areas of cell-substrate contact; portions of cells spanning troughs lacked focal adhesions and phosphotyrosine. Cells grown on the posted surfaces showed orthogonal arrays of microfilaments that conformed to the intersecting troughs between posts; stress fibers, however, were not observed. These cells either rested atop the posts or settled down onto the posts, with the posts apparently displacing cytoplasm and limiting the distribution of microfilament bundles to areas of basal contact. SEM observations confirmed that the posts penetrated the basal cell membrane surface, with the cell contents settling around the posts. Focal attachments and phosphotyrosine were similarly distributed in these cultures.

Discussion: This experiment demonstrated that parallel and intersecting grooves are capable of affecting the shape, orientation, cytoskeletal organization, and distribution of focal adhesions in 3T3 fibroblasts, extending our previous findings of these effects in rat tendon fibroblasts. The role of extracellular matrix in guiding this process, while not characterized, is not discounted. The limitation of kinase activity by physical substrate features is a novel finding and could shed light on mechanisms by which cell types respond differentially to substrates. Ultimately, we hope to uncover phenotypic differences in these properties between cell types that will direct the tissue response to implants in ways that improve the incorporation of and extend the functional life spans of the implants.

Acknowledgements: This work was aided by National Science Foundation SBIR phase I grant #9160684 and by Jersey City State College SBR grant #220251. Microgeometry molds were prepared by the Cornell Nanofabrication Facility.

Effects of Surface Microgeometry on Fibroblast Shape and Cytoskeleton

JC Grew, JL Ricci, AH Teitelbaum, JL Charvet.

Presented at the 23rd Annual Meeting of the Society for Biomaterials.
April 30-May 4, 1997. New Orleans, LA.

ABSTRACT

Introduction: Surface microgeometry influences tissue-implant interaction, although the interaction is poorly understood. Cellular contact guidance, a tissue response to surface microgeometry, profoundly influences cell growth and other behaviors. For example, on grooved surfaces, groove depth and width minima are required to affect cell shape and orientation and the direction of growth. Cytoskeletal organization reflects cell attachment, shape and orientation and likely contributes to these microgeometry-directed phenomena. We examined some properties of fibroblasts cultured on simulated biomaterials with various surface microgeometries. We studied rat tendon fibroblast (RTF) cells, because human fibrous tissue cells are among the first cells to contact implants. Fibrous implant encapsulation is influenced by surface roughness and microgeometry: roughening promotes thinner capsule development and, therefore, more intimate contact of bone cells and tissue with the implant and improved implant integration.

Methodology: RTFs from stock cultures derived from hind foot extensor tendons were grown on smooth (control) and patterned polystyrene substrates having parallel 2 or 12µm linear grooves or 8x50 or 80x50µm diamond-shaped islands separated by 3x3µm grooves. Substrates were solvent-cast on silicon molds and titanium oxide coated. Fifteen millimeter circular cutouts were fitted into 24-well plates, and wells containing inserts were seeded with 20,000 RTFs and fixed after 4 and 8 days in culture. Cell morphology was studied and recorded by scanning electron microscopy and by fluorescence microscopy of cultures stained with rhodamine phalloidin and anti-vinculin followed by a fluorescein-conjugated secondary antibody.

Results: The orientations and shapes of RTFs grown on control and patterned surfaces were consistently different. Cell orientation tended to be random in control cultures, but generally coincided with the directions of the linear grooves and the longer dimensions of the diamonds. RTFs grown on 2µm grooved and diamond-patterned substrates often bridged the grooves, attaching to elevated substrates. RTFs grown on 12µm grooves grew both within the grooves and on elevated surfaces, but rarely bridged grooves. RTFs grown on the larger diamond-patterned substrate often grew in clusters on elevated areas. RTFs grown on control surfaces were approximately round and symmetrical, extending short processes omnidirectionally from a central cell mass. RTFs grown on linear substrates more typically assumed a spindle shape, and extend processes perpendicular to the grooves only when spanning a narrow (2 or 3µm) groove or to establish lateral contact with groove walls (12µm grooves). Substrate microgeometry also affected the organization of microfilament bundles (stress fibers), which were aligned with the predominant direction of cellular orientation in cells grown on the patterned substrates. RTFs from control cultures typically showed microfilament bundles extending at miscellaneous angles throughout the cell cytoplasm. In all cells, vinculin was localized at microfilament bundle termini, as revealed by imunofluorescence microscopy, indicating points of cell-substrate attachment consistent with the presence of focal attachments.

Conclusions: This study showed that both the linear and diamond patterns are capable of influencing the orientation and cytoskeletal organization of fibroblast cells, extending previous observations of contact guidance effects based on substrate microgeometry on cell shape alteration and directional growth. RTFs, which vary from 3 to 10µm in width, frequently bridged 2 and 3µm grooves, suggesting that more pronounced surface features may be required to optimally control the growth of these cells. The results of this experiment differ from earlier reports of the growth of "dot" cultures prepared with cells suspended in a collagen gel. Seeded cultures appear to be less sensitive to microgeometry effects than dot cultures. Outgrowing dot culture cells probably migrate considerable distances across substrate surfaces. Grooves may thus serve as more substantial guides to migrating dot culture cells than to cells in seeded cultures, which settle and thereafter remain stationary. Continued experimentation and comparison of these models, particularly in cellular attachment to substrates, will yield additional insight into the behaviors of these cells on patterned substrates. For instance, it may prove possible to control the rate and direction of fibrous tissue growth at the tissue-implant interface, thereby optimizing the stability of these implants.

Acknowledgements: This work was aided by NSF SBIR phase I grant# 9160684. Microgeometry molds were prepared by the Cornell Nanofabrication Facility.

Cell Interaction with Microtextured Surfaces

JL Ricci, R Rose, JK Charvet, H Alexander, CS Naiman.
Presented at the Fifth World Biomaterials Congress.
May 29-June 2, 1996. Toronto, Canada.

Table 1: Cell growth and shape parameters

	Surface			
	Control (smooth)	1.75µm	6.5µm	12.0µm
Cell colony after 8 days, mm² (S.D.)	83.8 (11.0)	85.6 (5.6)	36.6* (4.7)	39.3* (6.1)
Cell attachment area, µm² (S.D.)	2666.4 (1534.9)	604.4 (247.5)	621.1* (250.0)	934.0* (493.1)
Cell eccentricity, length/width (S.D.)	2.1 (0.9)	6.0* (2.6)	6.7* (3.4)	7.3* (3.4)
Cell density, cells/mm² (S.D.)	912.8* (135.5)	667.6* (115.8)	715.3* (114.9)	676.0* (134.6)
Cell orientation (relative to grooves)	Random	>90% within ±40°	100% within ±20°	>95% within ±20°

**p<.05*

ABSTRACT

Introduction: It has long been recognized that implant surface microtexture can influence tissue interaction. In previous studies we have examined the *in vitro* interaction of connective tissue fibroblasts with a variety of defined surface microgeometries, including microgrooved, roughened and more complex surfaces. In most cases, these surfaces, while having similar composition, have different (and pronounced) effects on the rate and direction of growth of fibroblast cell colonies. The mechanism of surface microgeometry's effect on cell colony growth rate is unknown. This study investigated the effect of defined surface microgeometry on connective tissue cell colony density, cell attachment area (spreading), and cell shape. The results suggest a possible basic mechanism of surface microgeometry control of attached cell growth.

Materials and Methods: Rat tendon fibroblast (RTF) cells were grown as stock cultures from hindfoot extensor tendons from 14-day-old Sprague-Dawley rats. Second to fourth-passage cells, grown in Dulbecco's Modified Eagle's Medium containing penicillin-streptomycin and 10% fetal bovine serum were used for all experiments. Cell colonies were grown on these surfaces using a "dot" culture model similar to explant culture models. These cells were suspended in solubilized collagen (Vitrogen, Celltrix, Palo Alto, CA) and 2µL droplets containing 20,000 cells each were polymerized on the experimental surfaces, where they acted as sources of radiating cell colony growth. Light microscopy and image analysis methods were used to measure rate and direction of growth as well as cell density (cells/mm^2), cell attachment area (µm^2), cell orientation (relative to substrate orientation), and cell elongation (eccentricity, the ratio of cell length to cell width). For individual cell measurements, 30 cells of each experimental group were measured. Experimental substrates consisted of solvent-cast polystyrene surfaces, vapor-deposited with 60nm of TiO_2, molded from silicon wafer templates produced by optical lithography methods at the National Nanofabrication Facility at Cornell University (Ithaca, NY). Substrates consisted of mirror-smooth surfaces (controls) and square-wave microgrooves with ridges and grooves 1.75, 6.5 and 12µm in size. Results were analyzed for statistical significance using t-tests.

Results: All three microgrooved surfaces had a pronounced effect on cell colony growth, cell attachment area, cell eccentricity, cell density, and cell orientation (Table 1): they reduced cell colony growth and cell spreading, increased cell eccentricity (elongation), and effectively oriented the cells parallel to the surface. Cell density on all experimental surfaces was reduced relative to controls.

Discussion: Well-defined surface microgeometries with the tested dimensions are effective at orienting cells, changing cell shape, and reducing cell growth rates. It is well known that attachment-dependent cells must attach and spread to trigger cell division. The present results suggest that the growth inhibition effect demonstrated by these surfaces may be based on reduction of cell spreading by the surface microgrooves. These experiments suggest that observed differences in fibrous encapsulation of smooth vs. microtextured surfaces may be based on direct suppression of fibroblast spreading and growth by microtextures. These microgeometries have potential application as implant surfaces for control of tissue integration.

Acknowledgements: This work was funded by Orthogen Corporation through NSF SBIR Phase I award 9160684.

In Vitro Effects of Surface Roughness and Controlled Surface Microgeometry on Fibrous Tissue Cell Colonization

JL Ricci, J Charvet, R Sealey, I Biton, WS Green, SA Stuchin and H Alexander.
Presented at the 21st Annual Meeting of the Society for Biomaterials. March 18-22, 1995. San Francisco, CA.

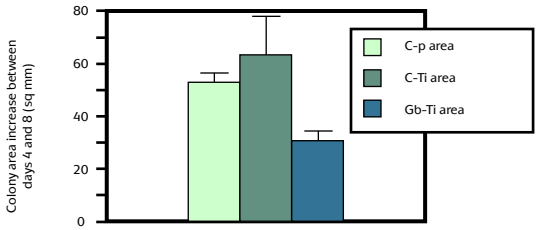

Figure 1. RTF cell colony growth on roughened (GB-Ti) and smooth (C-p and C-Ti) surface.

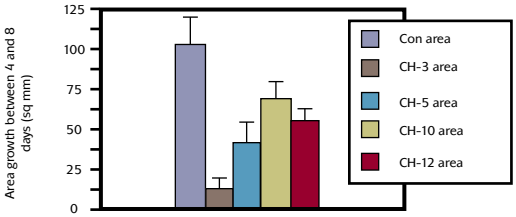

Figure 2. RTF cell colony growth on cross-hatched surfaces from 3 µm (CH-3) to 12 µm (CH-12) in feature size, and on smooth surface controls (Con)

ABSTRACT

Introduction: Soft tissue encapsulation of an implant has been found to correlate with the composition, surface chemistry, and surface microgeometry of the implant material. Surface microgeometry (or surface texture) of metal implants in bone has been shown to influence fibrous capsule formation. For example, smooth surfaces induce thicker fibrous capsule formation than roughened surfaces, suggesting that surface microgeometry influences fibrous tissue proliferation. We evaluated the *in vitro* response of rat tendon fibroblast (RTF) cell colonies, and human implant capsule fibroblast (HICF) cell colonies, from fibrous capsule tissue from around total hip replacement components, to surfaces roughened by blasting techniques, and to controlled surface microgeometries consisting of small square post projections with features from 3 to 12 µm in size.

Materials and Methods: RTF cells were grown from hind-foot extensor tendons of 14-day-old Sprague Dawley rats. HICF cells were grown from fibrous capsule tissue samples obtained from patients undergoing total hip revision, including removal of an uncemented hip prosthesis. The tissues, obtained from an area near the proximal stem, were grown as explants under sterile conditions to produce stock cell cultures. All cells were grown as stock cultures, mixed with solubilized collagen, and dispensed and polymerized to initiate "dot" cultures, consisting of 2µL dots each containing 20,000 cells, on all experimental surfaces. These cell-collagen dots acted as sources of cell outgrowth to form growing cell colonies. At 4 and 8 days, cell colonies were fixed, stained, and measured for area of growth using a video camera-equipped stereomicroscope connected to a computer image-processing/image-analysis system. Growth of the cell colonies was measured as area or diameter increase between 4 and 8 days. Roughened surfaces were produced by grit-blasting or bead-blasting of polystyrene culture plates. A masked area was used as a smooth control surface. These surfaces consisted of a range of feature sizes depending on blast medium. The media were similar to those used to texture metal orthopaedic implants and produced similar sized features. Controlled microgeometry substrates were molded in solvent-cast polystyrene from templates precision-fabricated using optical lithography methods at the National Nanofabrication Facility at Cornell University. All surfaces were sputter-coated with a 600-Å layer of TiO_2 to simulate an orthopaedic titanium alloy implant surface. The controlled microgeometry surfaces consisted of well-characterized, cross-hatched or checkerboard surface patterns consisting of square posts in 3, 6, 10 and 12µm feature sizes.

Results: All cell colonies showed consistent growth by day 4, with cell outgrowth observed at the periphery of the dot. Randomly oriented cells formed circular colonies on the control surfaces, and the roughened surfaces. The controlled microgeometry surfaces produced colonies with unusual shapes because of surface restriction of direction of growth. On an individual cell level, the cells were observed to orient along surface structures and in grooves between surface structures. On the smallest controlled microgeometries, each cell was observed to attach to the surfaces of several of the square posts. All of the experimental surfaces significantly inhibited cell colony growth in both types of cells. Significant cell growth inhibition was observed on the grit-blasted Ti-coated surface (GB-Ti) compared to the control Ti-coated surface (C-Ti) and the control untreated culture plate (C-p) as shown in Fig. 1 which represents RTF cell growth. The most efficient cell growth inhibition was observed on the 3µm cross-hatched surface (Fig. 2), although all of the cross-hatched surfaces caused significant inhibition of colony growth. Figure 2 also shows RTF cell colony data.

Conclusions: RTF and HICF cell colonies grown on roughened surfaces and on a series of controlled microgeometries exhibited pronounced inhibition of growth. The surfaces did not increase cell density in the colonies and the effect was not based on increased substrate surface area. The observed results represent the effects of cellular contact guidance – the ability of substrate microgeometry to influence cell orientation and migration – on overall growth of cell colonies. The observed effects of roughened surfaces and microgeometries on fibrous tissue cell growth, *in vitro*, may be related to the observation that roughened surfaces cause less fibrous encapsulation *in vivo*. If so, controlled microgeometry surfaces may be used to effectively suppress fibrous encapsulation.

Acknowledgements: This work was supported by Orthogen Inc., and was aided by a grant from the Orthopaedic Research and Educational Foundation.

1. Implant success rate is the weighted average of all published human studies on BioHorizons implants. These studies are available for review in this document and BioHorizons document number ML0130.

2. Human Histologic Evidence of a Connective Tissue Attachment to a Dental Implant. M Nevins, ML Nevins, M Camelo, JL Boyesen, DM Kim. *International Journal of Periodontics & Restorative Dentistry*. Vol. 28, No. 2, 2008.

3. The Effects of Laser Microtextured Collars Upon Crestal Bone Levels of Dental Implants. S Weiner, J Simon, DS Ehrenberg, B Zweig, JL Ricci. *Implant Dentistry*, Volume 17, Number 2, 2008. p. 217-228.

4. Clinical Evaluation of Laser Microtexturing for Soft Tissue and Bone Attachment to Dental Implants. GE Pecora, R Ceccarelli, M Bonelli, H Alexander, JL Ricci. *Implant Dent*. 2009 Feb;18(1):57-66.

5. Radiographic Analysis of Crestal Bone Levels on Laser-Lok® Collar Dental Implants. C Shapoff, B Lahey, P Wasserlauf, D Kim. *Int J Periodontics Restorative Dent 2010;30:129-137.*

6. The effects of laser microtexturing of the dental implant collar on crestal bone levels and peri-implant health. S Botos, H Yousef, B Zweig, R Flinton and S Weiner. *Int J Oral Maxillofac Implants* 2011;26:492-498.

7. Marginal Tissue Response to Different Implant Neck Design. HEK Bae, MK Chung, IH Cha, DH Han. *J Korean Acad Prosthodont*. 2008, Vol. 46, No. 6.

8. Bone Response to Laser Microtextured Surfaces. JL Ricci, J Charvet, SR Frenkel, R Change, P Nadkarni, J Turner and H Alexander. *Bone Engineering* (editor: JE Davies). Chapter 25. Published by Em2 Inc., Toronto,Canada. 2000.

9. Osseointegration on metallic implant surfaces: effects of microgeometry and growth factor treatment. SR Frankel, J Simon, H Alexander, M Dennis, JL Ricc*i. J Biomed Mater Res*. 2002;63(6): 706-13.

10. Surface Topography Modulates Osteoblast Morphology. BD Boyan, Z Schwartz. *Bone Engineering* (editor: JE Davies). Chapter 21. Published by Em2 Inc., Toronto, Canada. 2000.

11. Effects of titanium surface topography on bone integration: a systematic review. A Wennerberg, T Albrektsson. *Clin Oral Implants Res.* 2009 Sep;20 Suppl 4:172-84.

12. Histologic Evidence of a Connective Tissue Attachment to Laser Microgrooved Abutments: A Canine Study. M Nevins, DM Kim, SH Jun, K Guze, P Schupbach, ML Nevins. *International Journal of Periodontics & Restorative Dentistry.* Vol. 30, No. 3, 2010.

Direct Offices

BioHorizons USA
888-246-8338 or
205-967-7880

BioHorizons Canada
866-468-8338

BioHorizons Spain
+34 91 713 10 84

BioHorizons UK
+44 (0)1344 752560

BioHorizons Germany
+49 761-556328-0

BioHorizons Australia
+61 2 8399 1520

BioHorizons Chile
+56 2 361 9519

Distributors

For contact information in our 85 markets, visit www.biohorizons.com

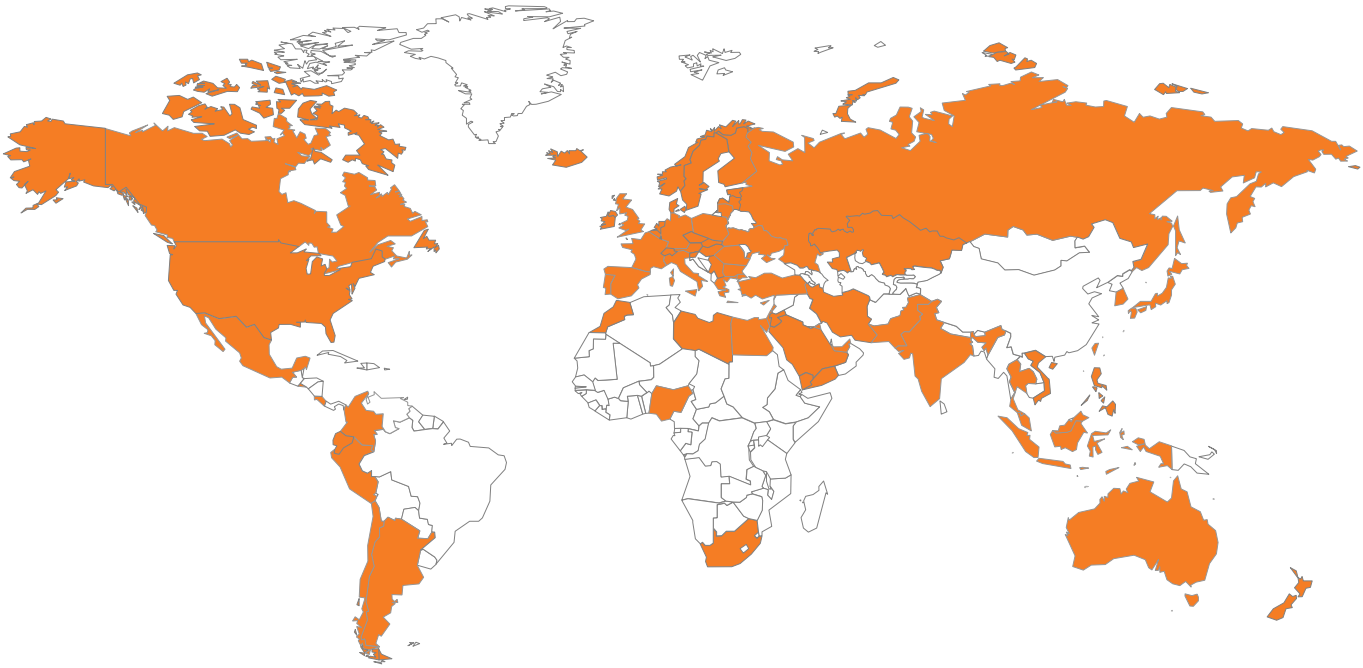

shop online at

www.biohorizons.com

ML0606

REV F JAN 2012